NATIONAL ENERGY TECHNOLOGY LABORATORY

Integrated Transpiration and Lattice Cooling Systems Developed by Additive Manufacturing with Oxide-Dispersion Strengthened (ODS)Alloys

Minking Chyu, Albert To
University of Pittsburgh

Bruce S. Kang
West Virginia University

Outlines

- ***Background, Challenges, Objectives, Benefits of Technology, Research Task Plans***
- *Additive Manufacturing Processes*
- *Heat Transfer Results: Transpiration Cooling*
- *Heat Transfer Results: Lattice Cooling*
- *ODS Powder Development*
- *Summary*

Need for Turbine Cooling

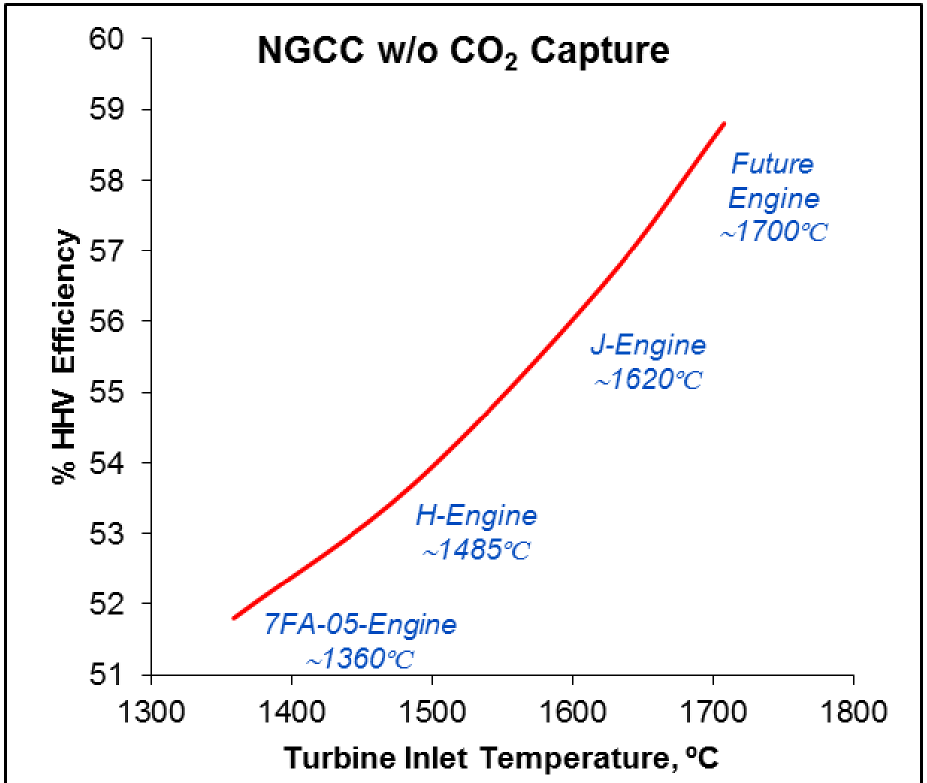

– W.Shelton, NETL Communication December 2011 –

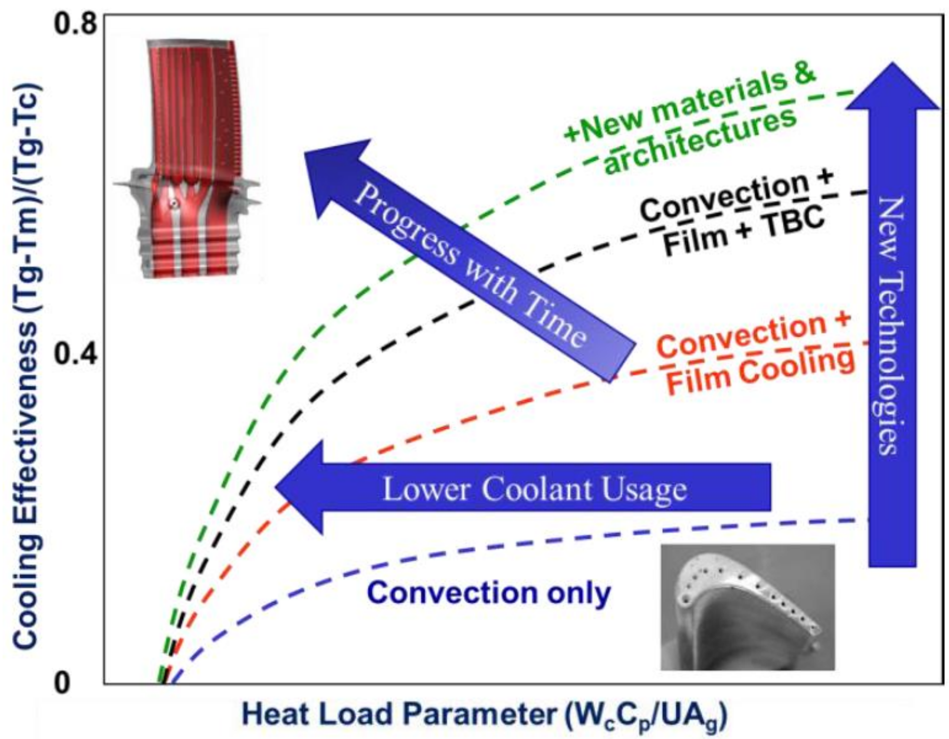

Bunker RS. Evolution of Turbine Cooling. ASME. Turbo Expo: Power for Land, Sea, and Air, Volume 1: Aircraft Engine; Fans and Blowers; Marine; Honors and Awards ():V001T51A001. doi:10.1115/GT2017-63205.

Airfoil metal temperature distributions (in K)
h_c=3000W/m²-K

- ***Gas temperature: Hydrogen-fired turbine (~1430ºC)***

Near surface 'skin cooling' or 'double-wall' internal cooling **arrangement leads to a significant reduction of metal surface temperature, ~50 – 100°C, compared to conventional serpentine cooling designs**

One key will be the marriage of design and manufacturing to bring about the concurrent use of engineered micro cooling or transpiration, with the ability of additive manufacturing. If successful, this combination could see a further 50% reduction in coolant usage for turbines.

Proposed Technologies

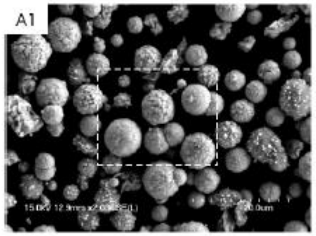

ODS

Enhanced oxidation resistance and high temperature strength

Advanced Additive Manufacturing

Intricate Heat Transfer Enhancement Features

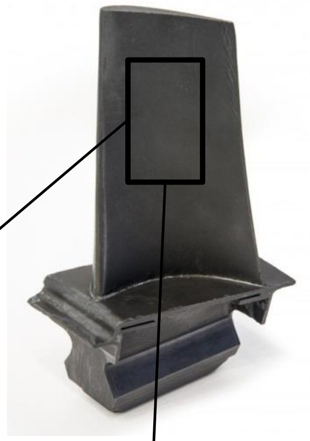

Near Surface Embedded Cooling Channel (NSECC)

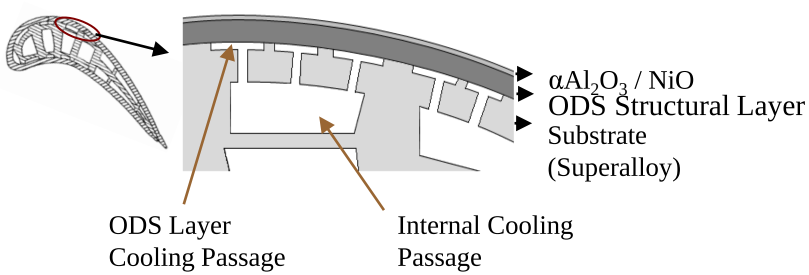

Integrated Transpiration and Lattice Cooling Systems

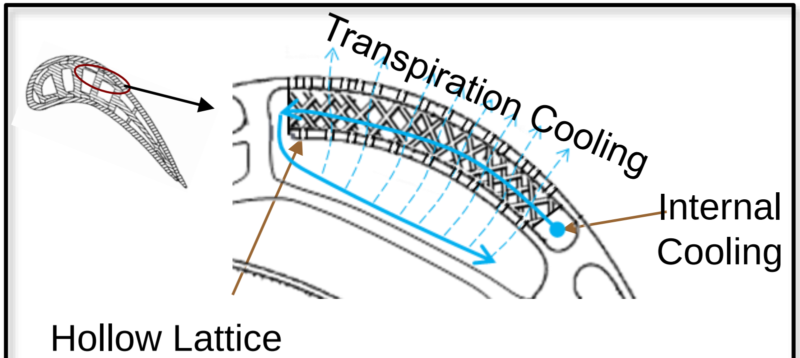

ODS with AM

- *Both internal and external protection.*
- *Oxidation Resistance*
- *Realized with additive manufacturing*

Novel ODS Surface Coating

- *Ultra-High Temperature (1200℃) Strength: thinner outer wall for better cooling*
- *Oxidation Resistance*
- *Higher turbine inlet temperatures*

Enhanced Heat Removal

- *NSECC: high internal heat transfer and higher coolant flow near hot end wall.*
- *Lattice and transpiration combined conjugate cooling: ~2x of state-of-the-art film cooling.*

Project Work Breakdown Structure

Goal: Enhanced Oxidation Resistance and Thermal Protection of Turbine Blades

ODS Powder Fabrication and Characterization
- MCB/BM for powders fabrication
- Characterization

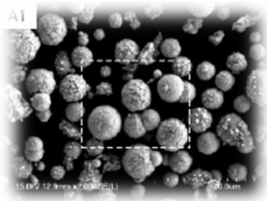

Cooling Geometry Design
- Transpiration and Lattice Geometry development and optimization

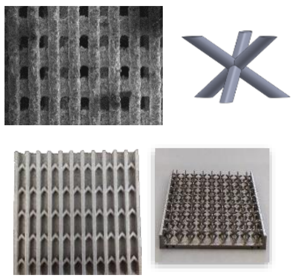

Lab-Scale Heat Transfer Characterization
- CFD modeling & steady state and scaled TLC testing
- Mini/micro scale cellular units

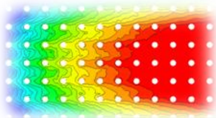

Thermal Cyclic Testing
- In-situ non-destructive micro indentation facility
- Thermal Cyclic Tests, Micro-hardness

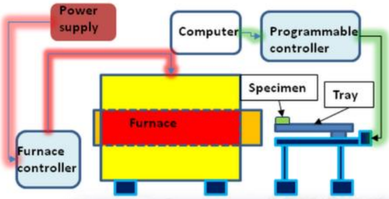

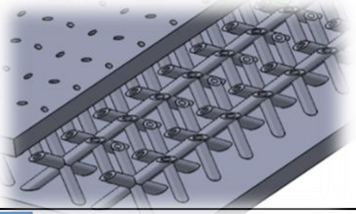

High Temperature Heat Transfer Characterization
High Temperature, Pressurized Testing (NETL)

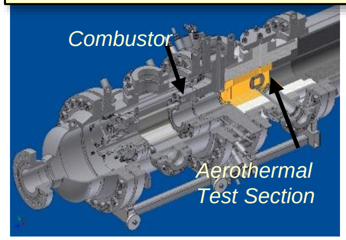

Process Optimization to Fabricate ODS Transpiration and Lattice Structures
- DMLS, BJT printing parameters
- Posting printing characterization
- OM, SEM

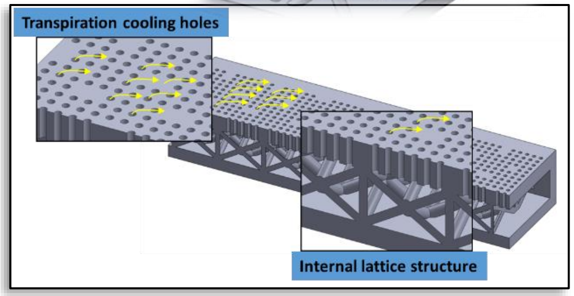

Milestones

- All milestones to be completed by COVID lockdown were on schedule
- Milestones E, F, and H moved to 2021 with one-year no-cost extension

Milestone Title	Planned Date	Verification Method
A - Identify prototypes for integrated transpiration and internal cooling	6/30/2018	Prototypes geometries will be generated through the original optimization algorithm, and CFD simulation should be conducted for each geometry.
B - Identify optimal configurations for integrated transpiration and internal cooling	9/30/2019	Systematic experimental tests should be conducted to proof the cooling effectiveness of the optimal geometry.
C - Integrate new unit types into the optimization Algorithm for ODS lattice structure	12/30/2019	Mechanical and heat transfer property of new lattice unit type should be obtained and input into the optimization algorithm. Several optimization cases should be conducted to proof the reliability of the algorithm.
D - Identify the capability of AM equipment to print ODS Structure	9/30/2018	The capability of printing ODS structures should be identified for the AM equipment at Pitt. Decision should be made which AM equipment is the most suitable to fabricate ODS lattice structure.
E - Develop Successful approach to make ODS Structure for integrated transpiration and internal cooling	5/31/2021	Complete the fabrication of ODS structures with complex lattice geometry. Microstructure inspection should be conducted using OM and SEM.
F - Complete high temperature experiments for integrated cooling structures made from ODS	9/30/2021	Heat transfer analysis will be conducted for the data obtained under high temperature. SEM characterization should also be included to exam the microstructure of ODS after high temperature operation.
G - Develop Successful approach to produce ODS powder suitable for additive manufacturing and lattice structures	9/30/2019	SEM and TEM characterization should be conducted to identify the sphericity, microstructure and size distribution of ODS powder.
H - Complete thermal cyclic loading tests	5/31/2021	Optical micrographs, SEM and nondestructive micro-indentation tests should be conducted to proof the long term stability of ODS material.

Benefits of Technology to the DOE Turbine Program

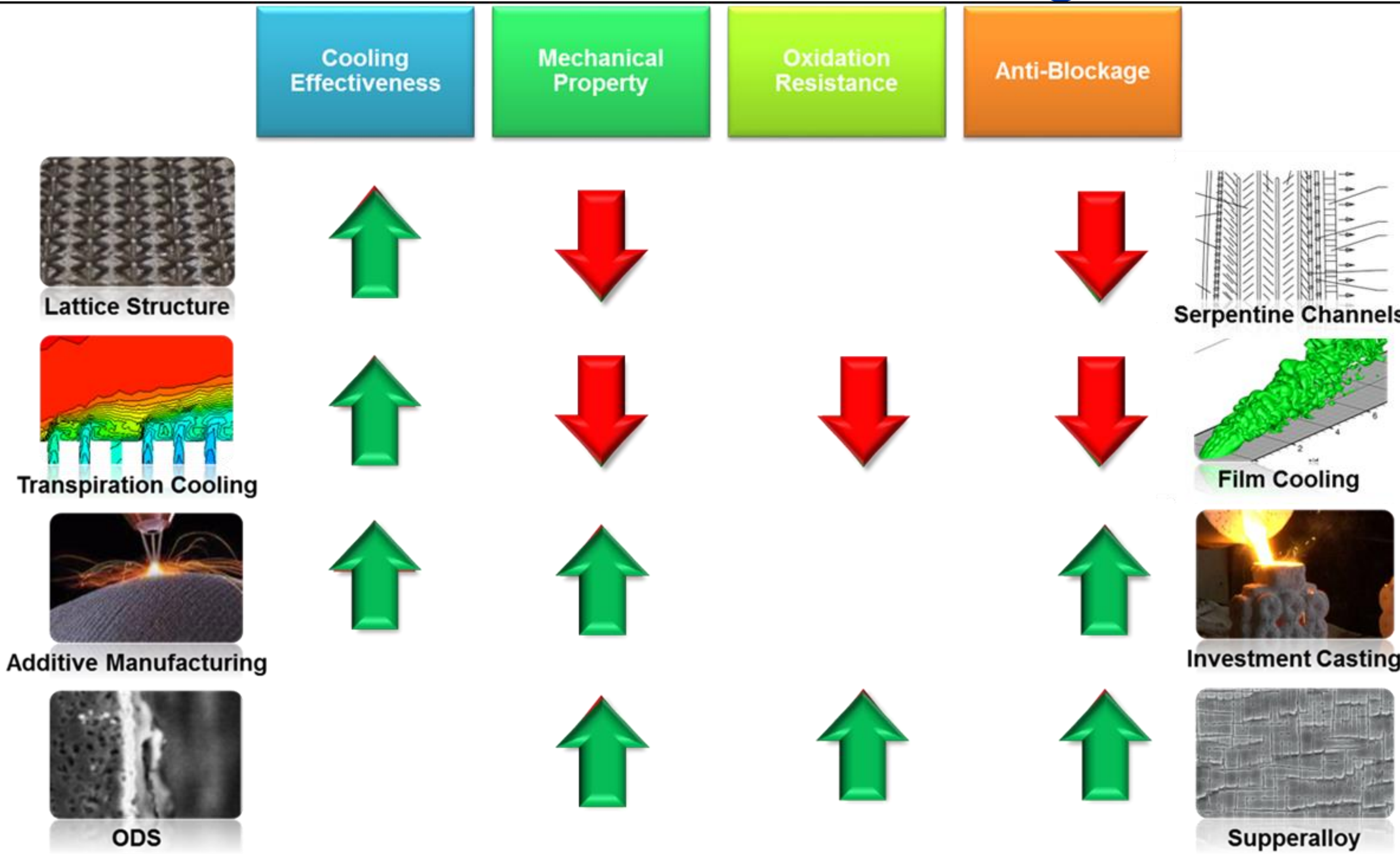

- ❑ Technical advancement ❑ Turbine industry ❑ Knowledge base ❑ Additive manufacturing promotion

Outlines

- Background, Challenges, Objectives, Benefits of Technology, Research Task Plans
- **Additive Manufacturing Processes**
- Heat Transfer Results: Transpiration Cooling
- Heat Transfer Results: Lattice Cooling
- ODS Powder Development
- Summary

AM Processes

Bind Jetting (EXOne)

Pros: geometry free
cons: high porosity

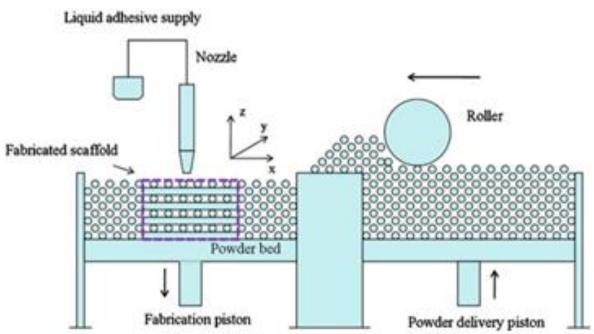

Powder Bed Fusion (EOS)

Pros: complex geometry
cons: single material

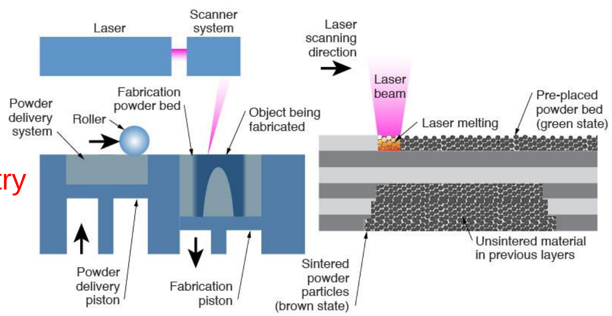

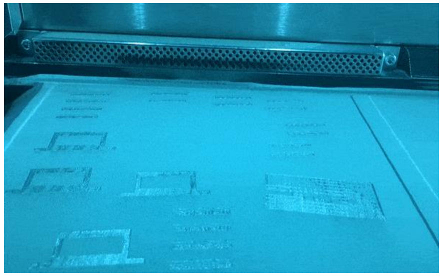

Direct Energy Deposition (LENS)

Pros: multiple materials
cons: no overhangs or unsupported structure

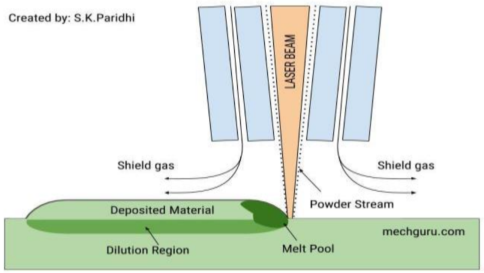

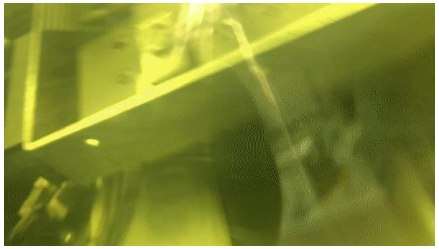

As metallic additive manufacturing technologies advance significantly over the recent past, complex metal products, such as turbine components, can be manufactured by this innovative technology.

ODS Coupons using DMLS

- ➢ Powder bed fusion process using laser
- ➢ Well developed process parameters for Inconel superalloys
- ➢ Challenges regarding ODS powder process development to be mitigated by systematic study

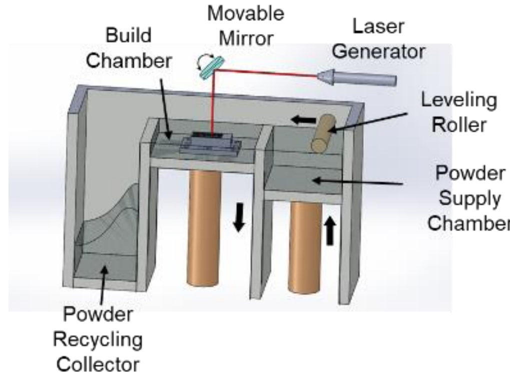

EOS M290

- **Laser Power**: 400W
- **Laser Focal Diameter**: 100μm
- **Scan Speed:** up to 7m/s
- **Printing Material:** Inconel 718 （similar composition to ODS)

- ➢ Fabricated coupons (In718)

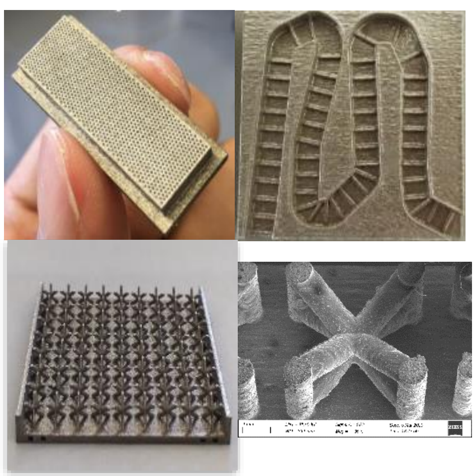

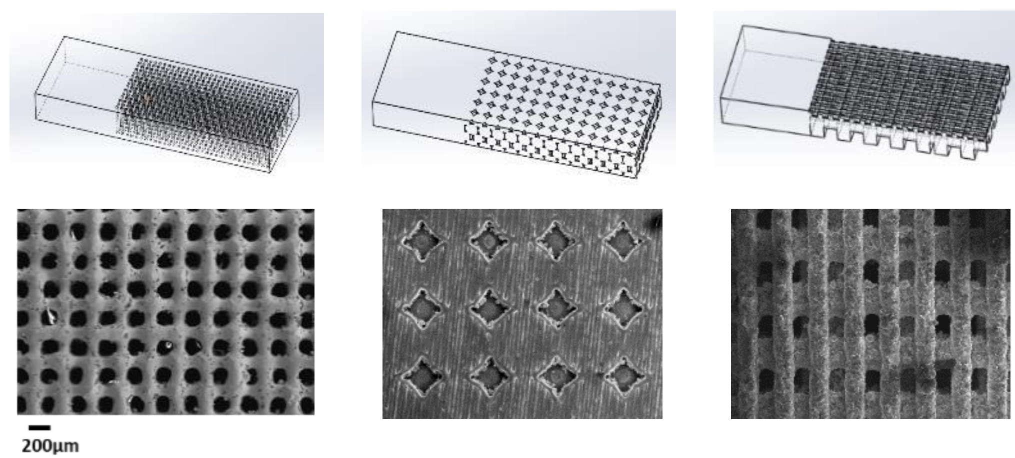

Outlines

- Background, Challenges, Objectives, Benefits of Technology, Research Task Plans
- Additive Manufacturing Processes
- **Heat Transfer Results: Transpiration Cooling**
- Heat Transfer Results: Lattice Cooling
- ODS Powder Development
- Summary

Transpiration Cooling – Introduction

➢ Concept: The coolant was forced through a porous wall or multiple micro-cooling channels to form an insulating layer of coolant film between the outer wall surface and hot stream.

Conventional Film Cooling

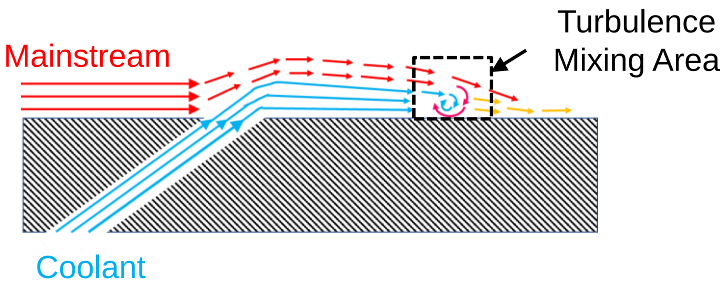

- "Lift-off" of the film due to jet momentum at the outlet
- Film protection weakened by turbulence mixing

Transpiration Cooling

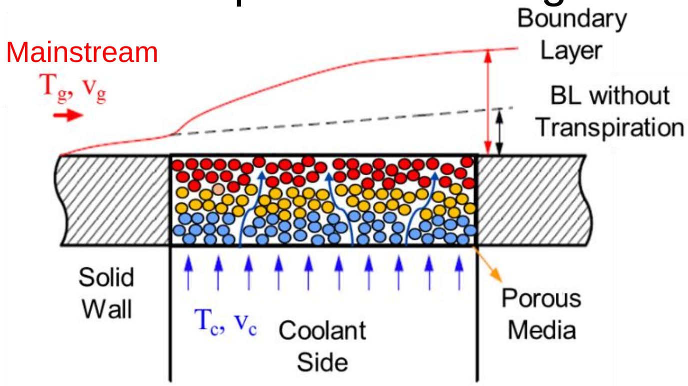

- Uniform coolant film coverage
- Enhanced heat removal ability due to higher inner-wall heat transfer

➢ Challenges

- Oxidation due to Vortex Mixing with Hot Gas
- Mechanical Strength Concern with Porous Media
- Manufacturing Difficulties

ODS:
- High Anti-oxidation Resistance
- High Temperature Mechanical Strength

AM:
- Comparable Strength with Casting
- Complexity and Design Freedom
- Fast and Low-cost Fabrication for Intricate Features

Transpiration Cooling – Surface Heater

➢ Surface heater fabrication

1. SLA printed resin samples with low thermal conductivity
    - Reduction of conductive heat loss
2. Micro-lithography fabrication for surface heater
    - Direct deposition of silver coil onto the target surface
    - No blockage/plugging of the outlets

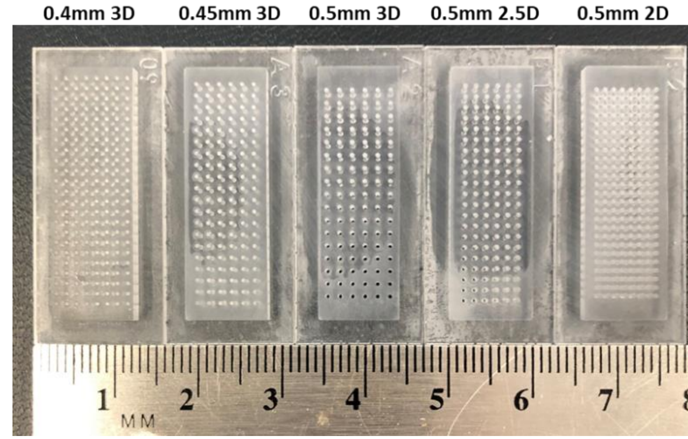

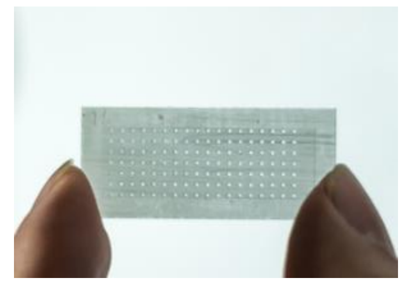

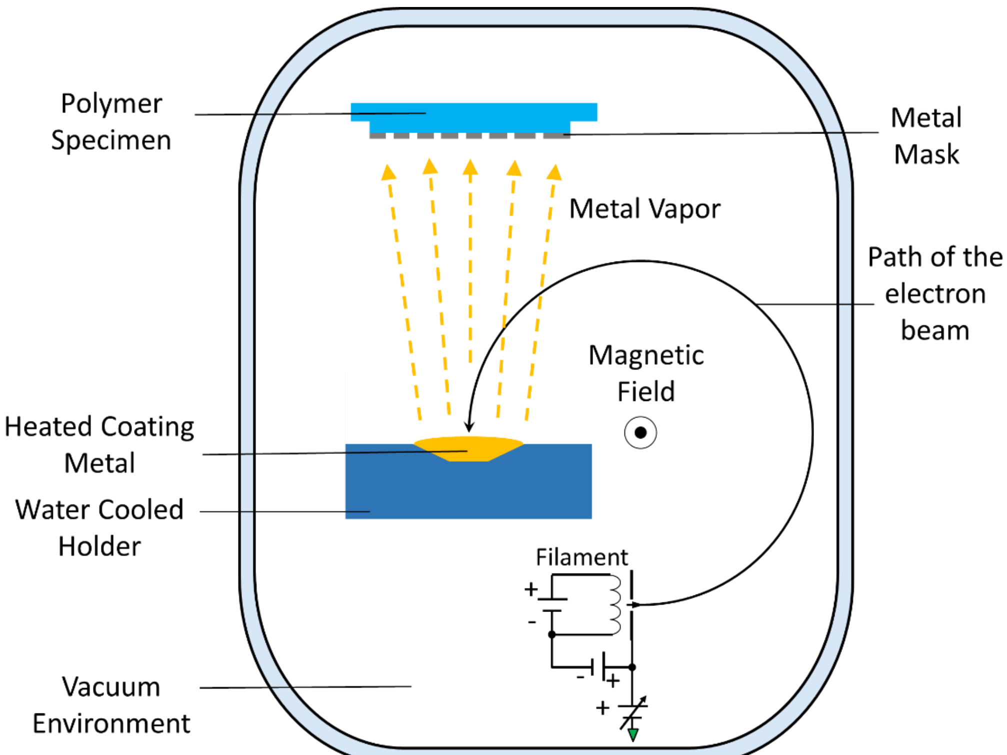

- *Plassys Electron Beam Evaporation System*

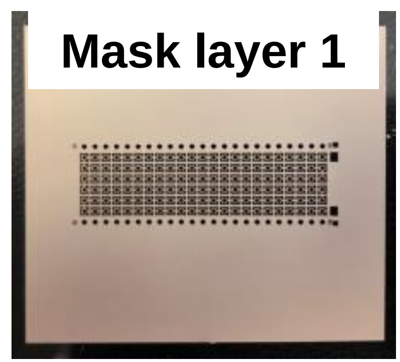

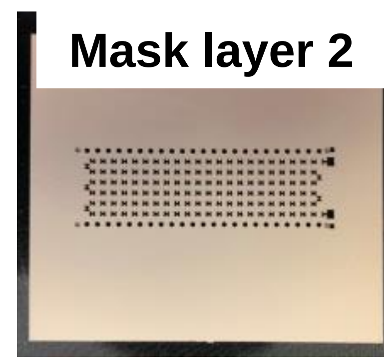

- *Photo Sciences, Inc.*

Transpiration Cooling – Wind Tunnel Test

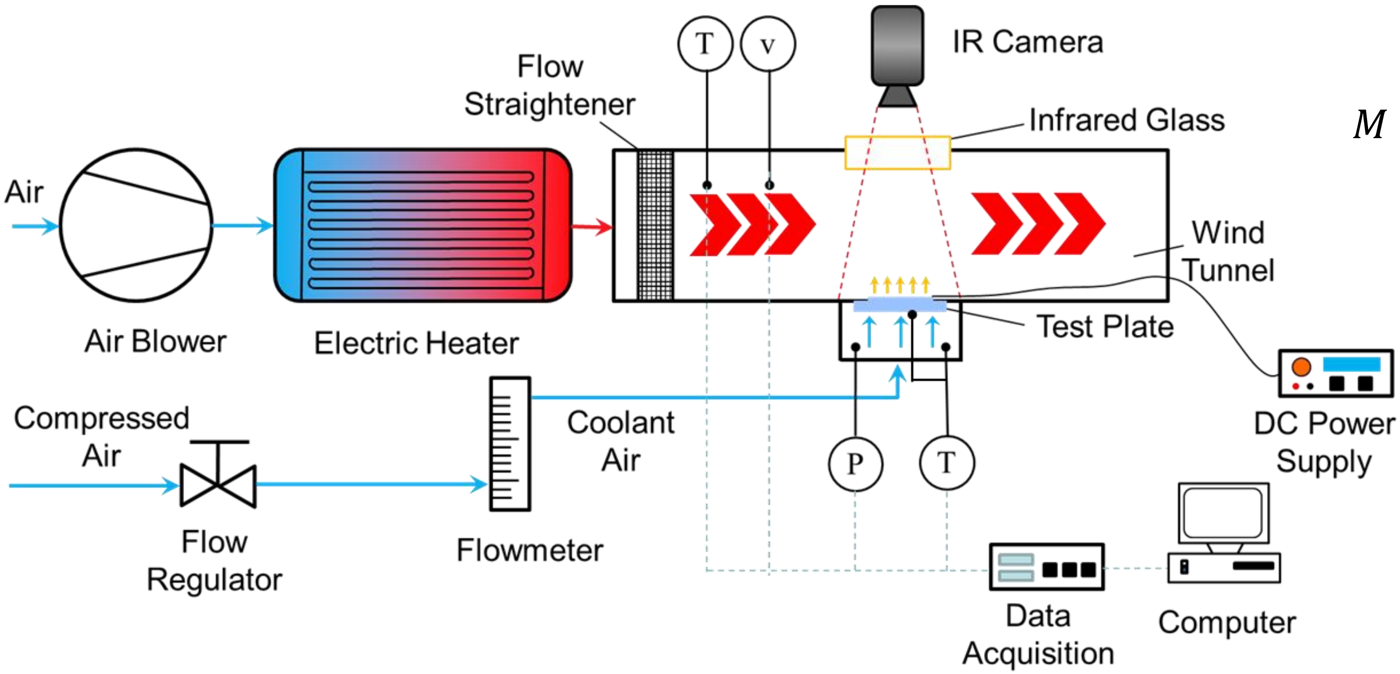

$$M = \frac{\rho_c u_c}{\rho_g v_g}$$

- **Heat transfer coefficient test:**

1. Blowing Ratio: M = 0.125, 0.25, 0.5
2. Coolant Temperature: T_c = 35 ℃
3. Mainstream Temperature: T_g = 35 ℃
4. Mainstream Velocity: v_g = 11m/s (Re_g=98,000)
5. Heater power on for h_f: 0.2W
6. No coolant injection to obtain h_0

- **Adiabatic cooling effectiveness test:**

1. Blowing Ratio: M = 0.125, 0.25, 0.5
2. Coolant Temperature: T_c = 21 ℃
3. Mainstream Temperature: T_g = 50 ℃
4. Mainstream Velocity: v_g = 11m/s (Re_g=98,000)
5. Heater power off for T_{aw}

Transpiration Cooling – Adiabatic Cooling Effectiveness

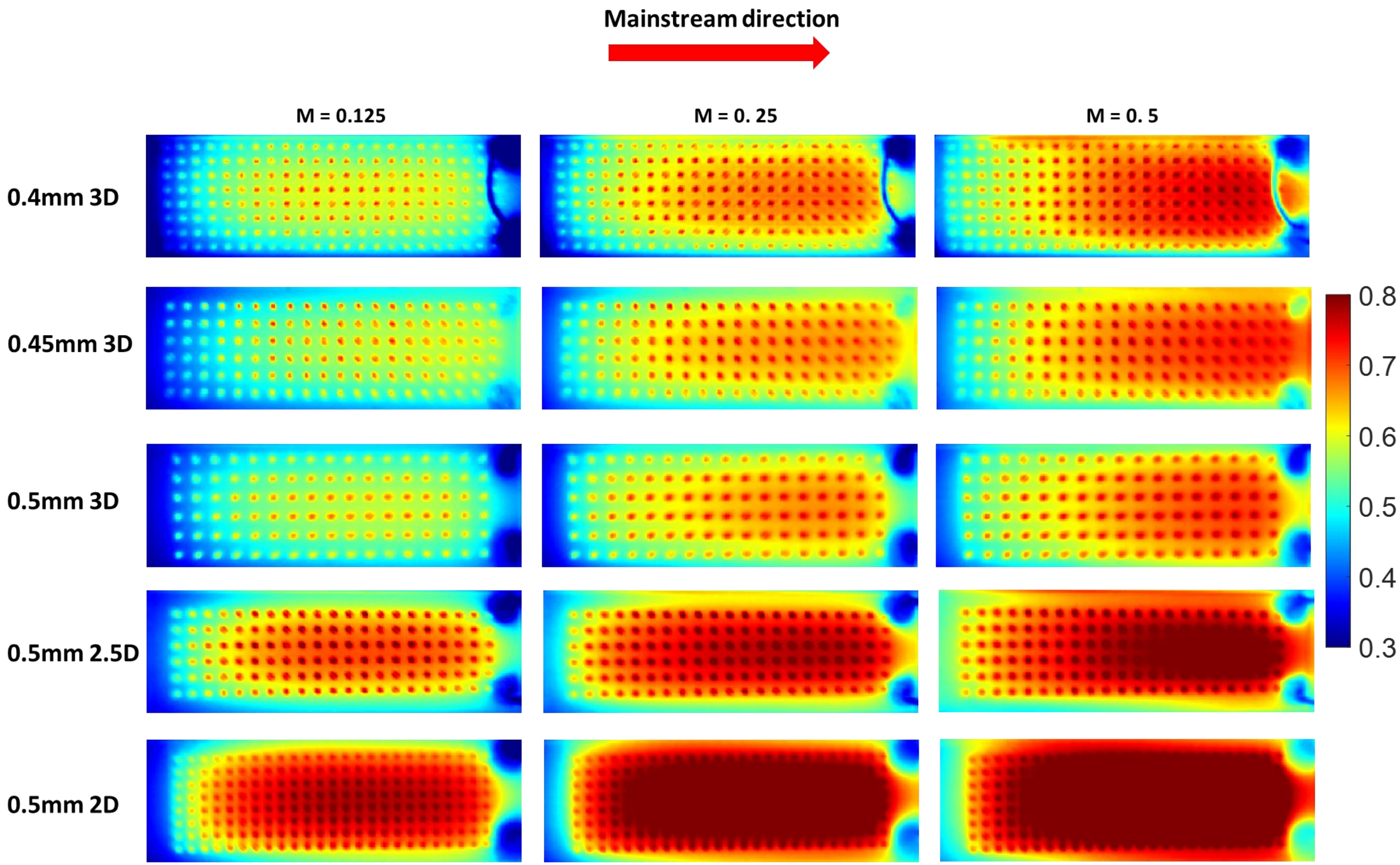

- Higher blowing ratio leads to higher cooling effectiveness
- For a given pitch-to-diameter ratio, smaller hole size leads to higher cooling effectiveness
- For a given hole size, smaller pitch-to-diameter ratio leads to higher cooling effectivenss

Transpiration Cooling – Adiabatic Cooling Effectiveness

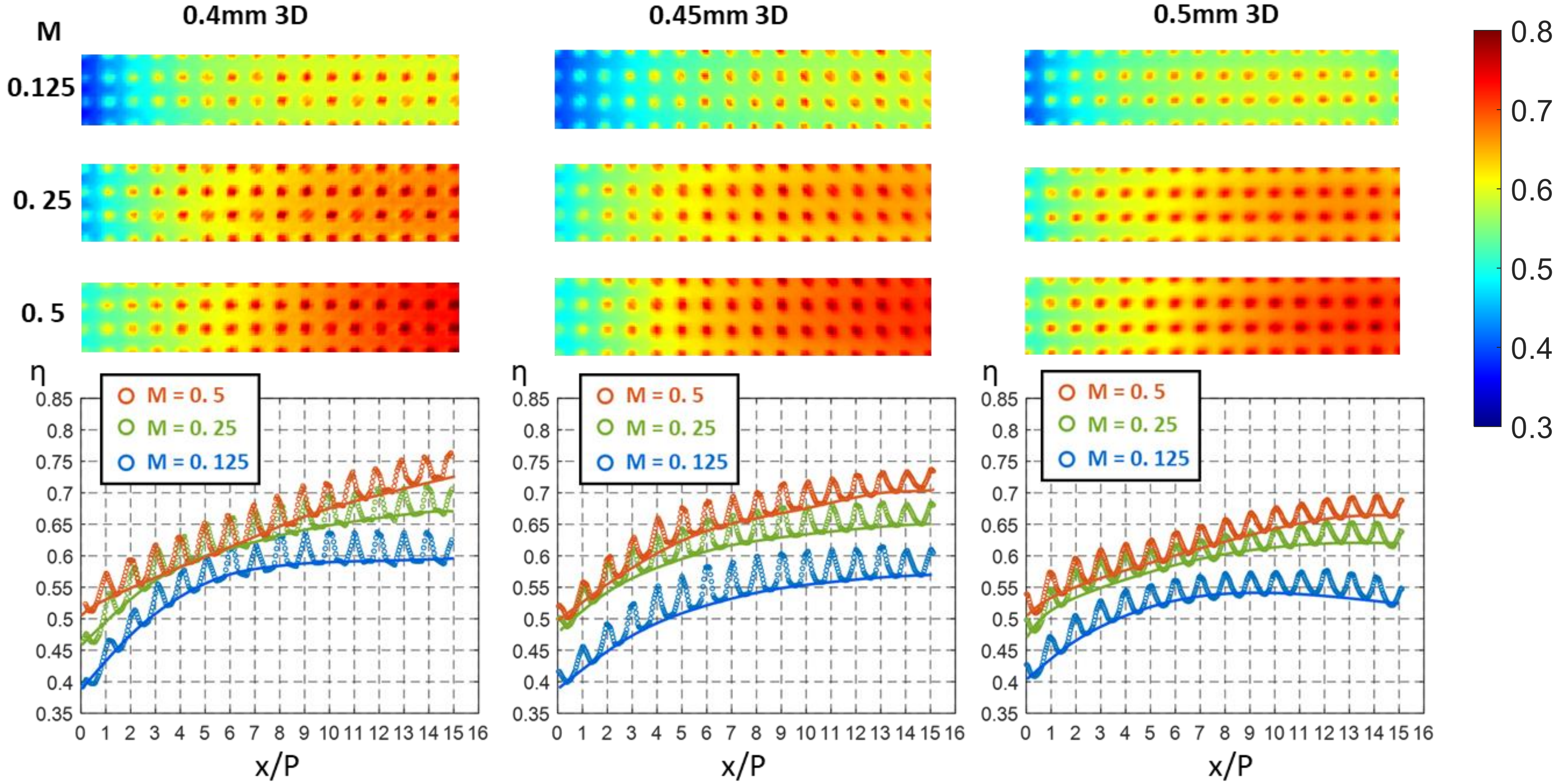

- Spanwise-averaged, streamwise-resolved cooling effectiveness.
- Effects of blowing ratio and hole size, with a given pitch-to-diameter ratio
- The impact of increasing blowing ratio from 0.25 to 0.5 is not as significant as the increase from 0.125 to 0.25

Transpiration Cooling – Adiabatic Cooling Effectiveness

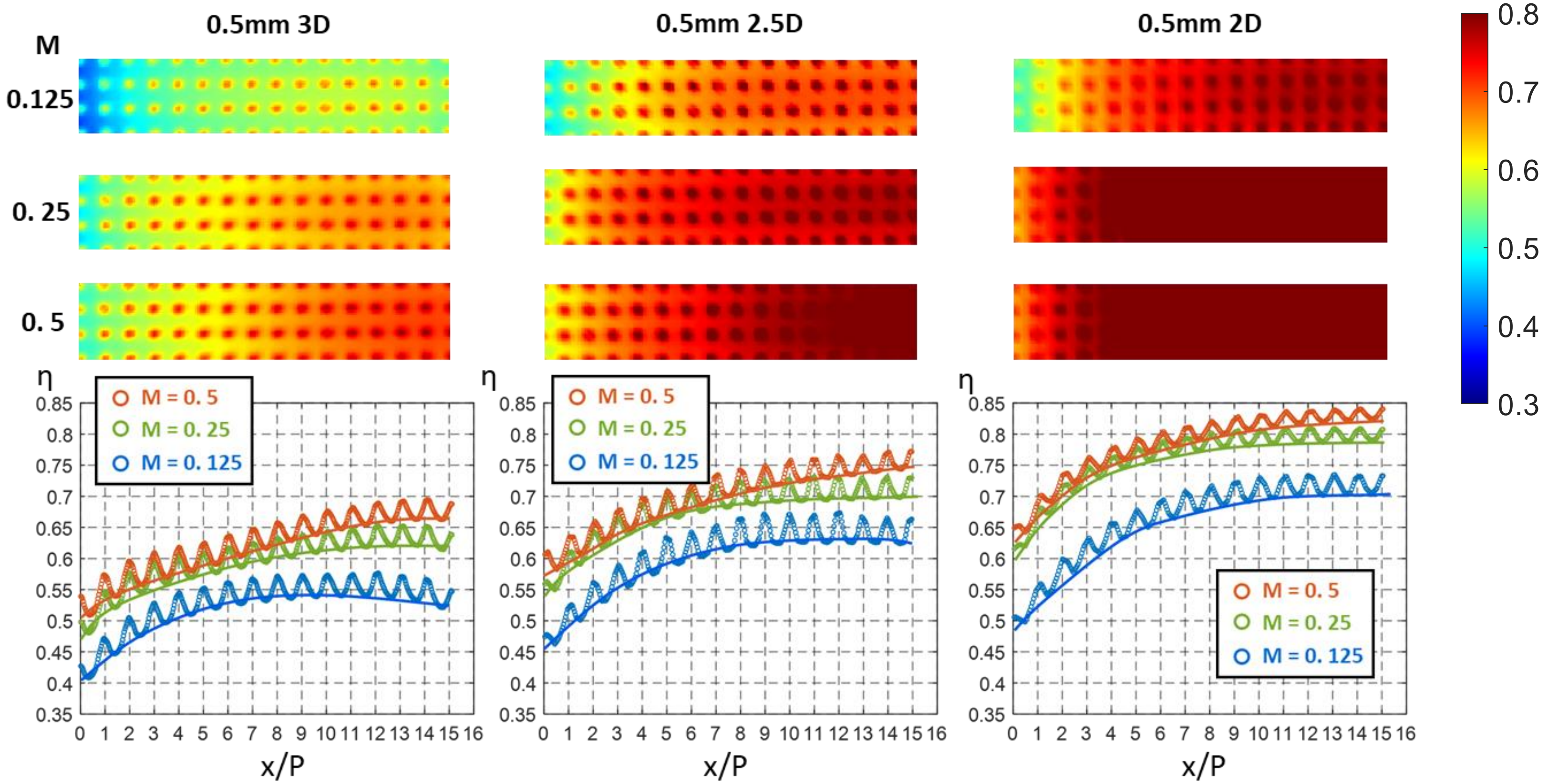

- For a given hole size, smaller hole pitch-to-diameter ratio leads to higher cooling effectiveness
- The impact of increasing blowing ratio from 0.25 to 0.5 is not as significant as the increase from 0.125 to 0.25

Transpiration Cooling – HTC

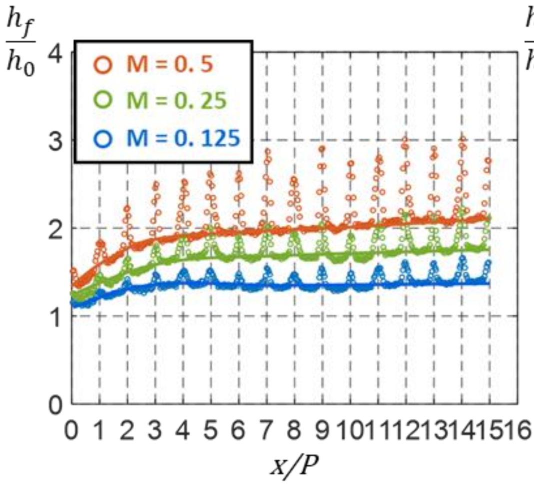

D=0.4mm, P=3D

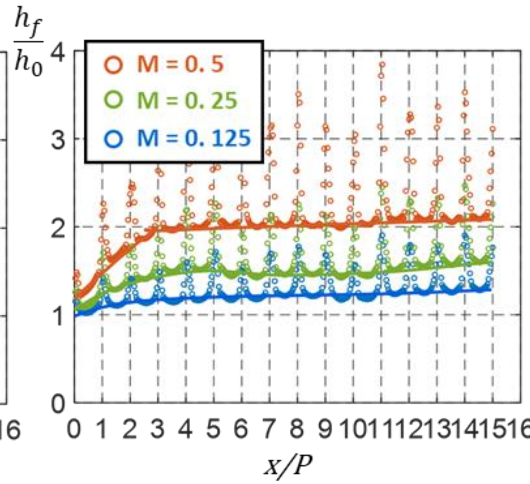

D=0.45mm, P=3D

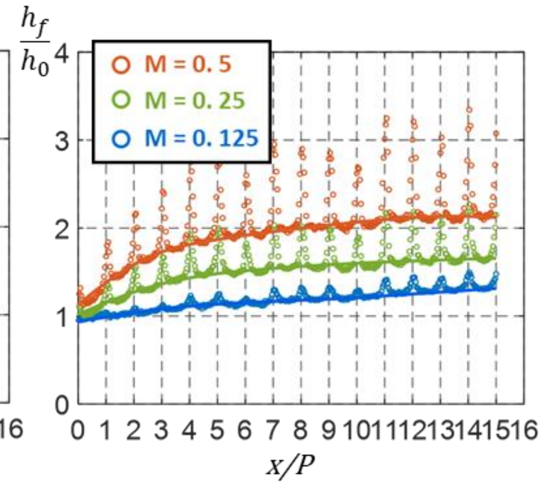

D=0.5mm, P=3D

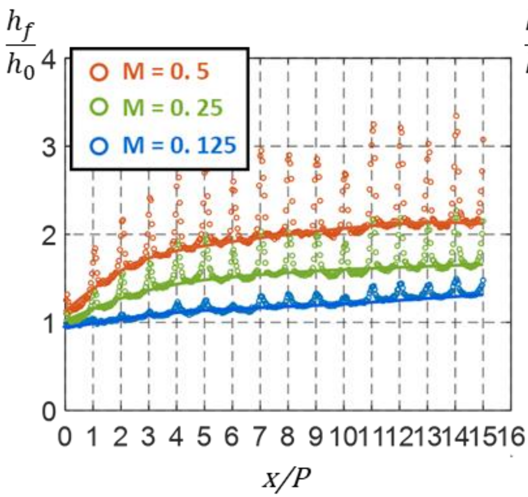

D=0.5mm, P=3D

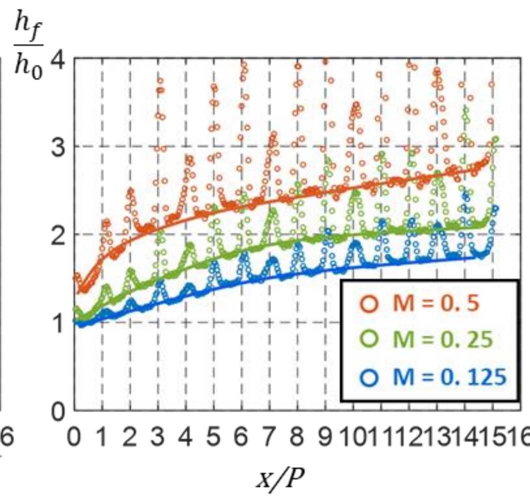

D=0.5mm, P=2.5D

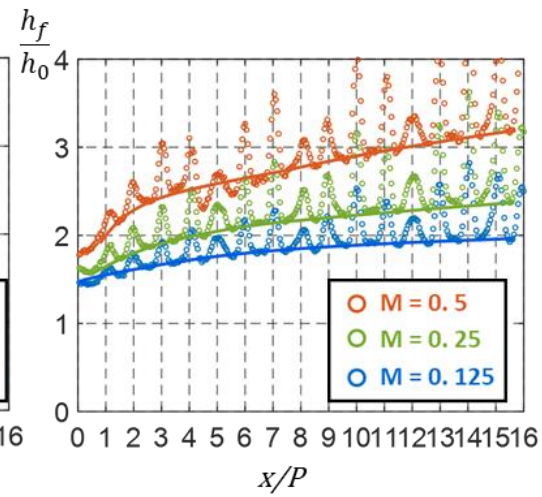

D=0.5mm, P=2D

- HTC increases with blowing ratio
- For a given pitch-to-diameter ratio, HTC is insensitive to hole size
- Smaller pitch leads to higher HTC, due possibly to interactions of neighboring coolant jets

Comparison with film cooling data in literature

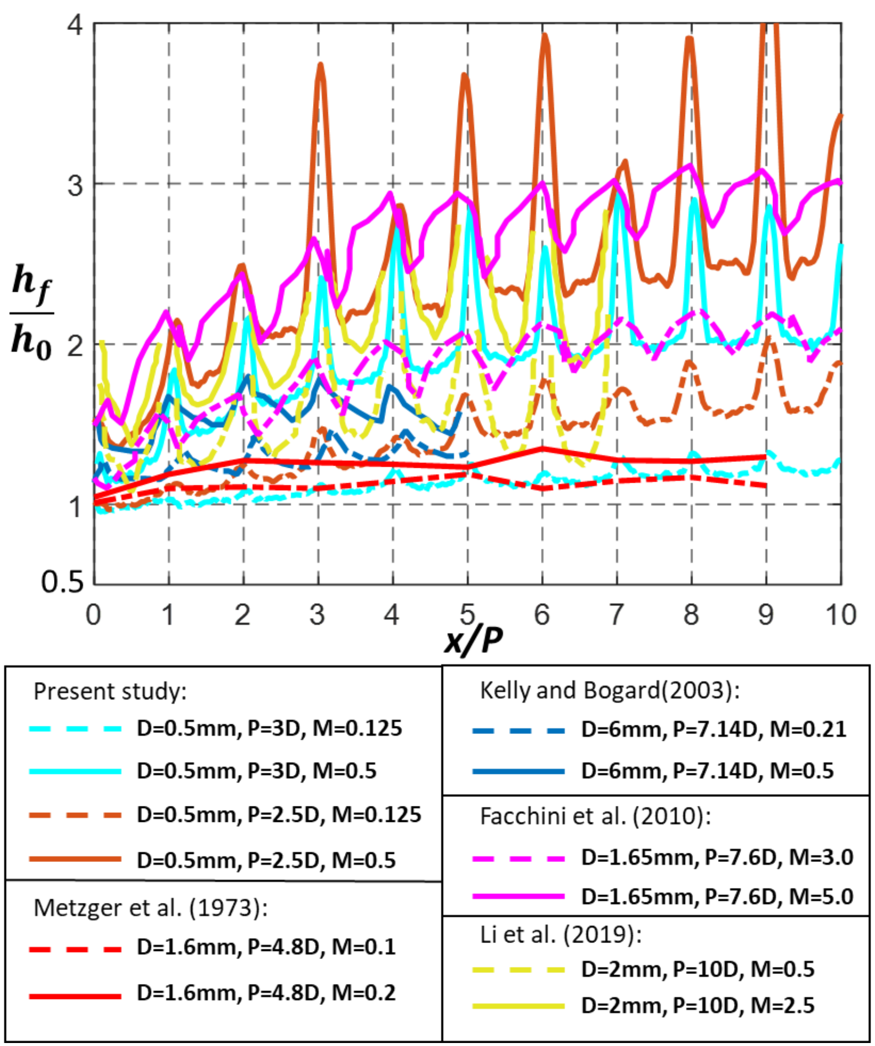

<u>M = 0.125 of transpiration cooing:</u>

- The transpiration cooling case of (D = 0.5mm, P =3D) is close to Metzger's case of M = 0.1, which means low momentum of the coolant injection hardly elevates HTC.
- For smaller pitch P = 2.5D, the HTC ratio increases, getting close to Kelly's data at blowing ratio of 0.21.

<u>M = 0.5 of transpiration cooing:</u>

- The transpiration cooling case of (D = 0.5mm, P = 3D) is close to Facchini's case of M = 3.0 and Li's case of M = 2.5, indicating significant turbulence intensity at the target surface
- For smaller pitch P = 2.5D, the HTC ratio gets even higher, getting close to Facchini's case of M = 5.0, the denser jets ejection significantly elevated the HTC at the target surface.

Comparison with film cooling data in literature

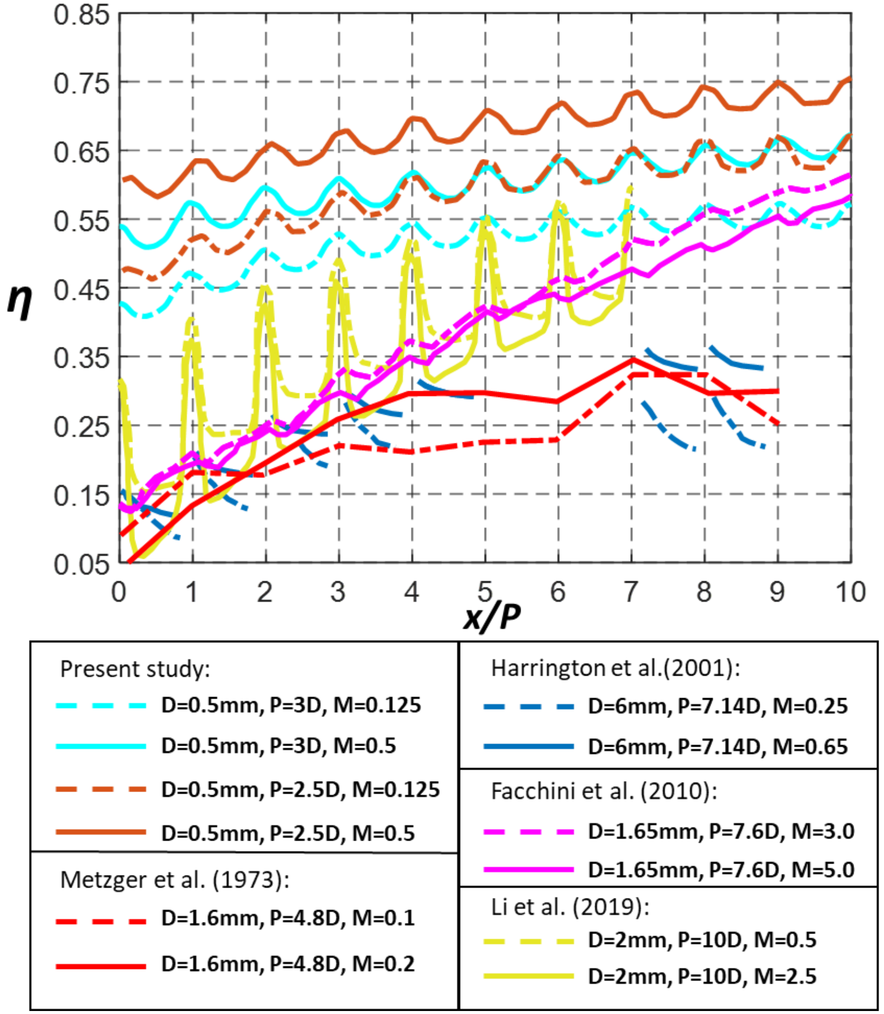

- η of transpiration cooling is significantly higher than multi-row film cooling
- More uniform and better coolant protection in the developing region of the first a few rows
- The impact of injecting more coolant (larger blowing ratio) is more pronounced for transpiration cooling structures

Outlines

- *Background, Challenges, Objectives, Benefits of Technology, Research Task Plans*
- *Additive Manufacturing Processes*
- *Heat Transfer Results: Transpiration Cooling*
- ***Heat Transfer Results: Lattice Cooling***
- *ODS Powder Development*
- *Summary*

Approaches to Fabricate ODS Lattice Structures

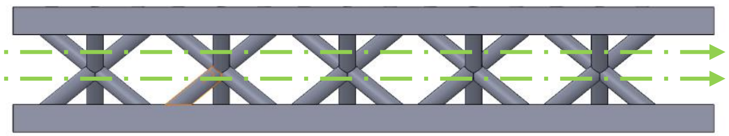

Internal Cooling with Macro Scale Lattice (Phase 1)

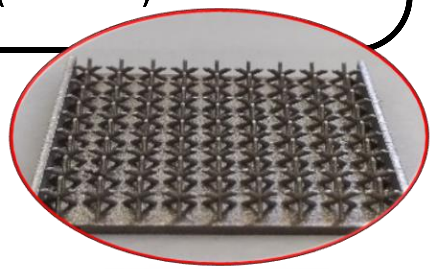

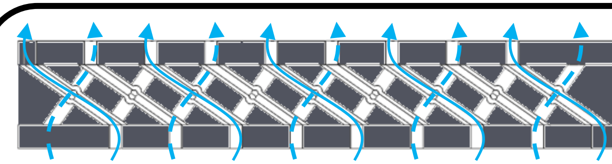

Transpiration Cooling with Micro Scale Lattice (Phase 2)

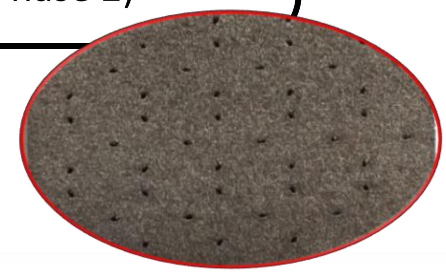

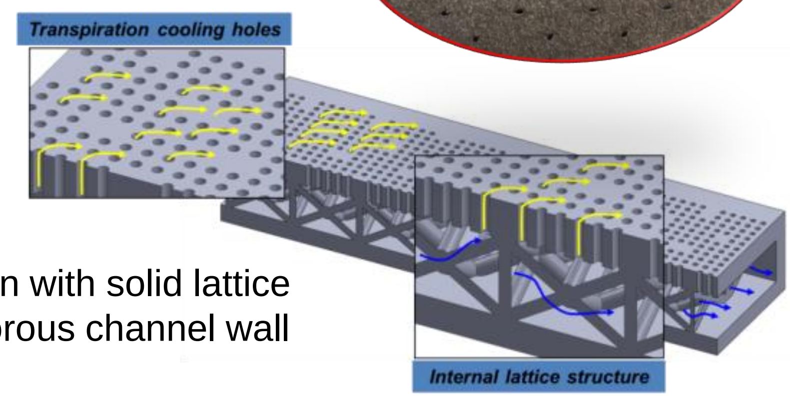

Coupon with solid lattice and porous channel wall

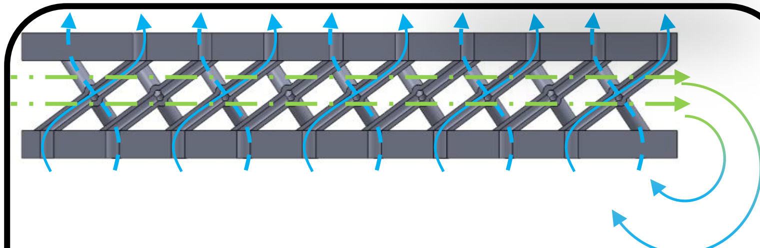

Combined ODS Internal and External Cooling with Multi-scale Lattice (Phase 3)

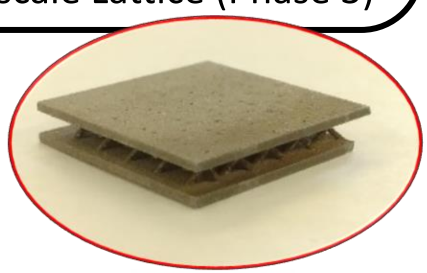

Challenges:

- AM process parameters for ODS
- Controlling dimension change and deformation
- Identify minimum limitation of pore diameters

Lattice Heat Transfer Characterization

Objective: Design highly efficient and manufacturable integrated transpiration and internal cooling which has an overall averaged cooling efficiency of more than 0.6.

- Internal heat transfer characterization with macro-scale lattice (Phase 1)
- Integrated with transpiration cooling with micro-scale lattice (Phase 2)

Approach

- Identification of candidate transpiration and lattice geometries
  - Transpiration: Candidate geometries from transpiration experiments
  - Lattice: Unit cell geometries, porosity, unit cell arrangement
- Experimental and numerical iteration
  - Experimental studies on cooling effectiveness
  - CFD to obtain flow fields
- Integrated design
  - Combining promising transpiration and lattice designs together to get high cooling effectiveness of more than 0.6
- Lattice optimization for improved thermal fluid enhancement characteristics

Internal Cooling with Macro Scale Lattice (Phase 1)

Overview of unit cells under investigation:

Advantages
- Provide structural rigidity
- High heat transfer surface area
- Promote turbulence in the bulk flow

Kagome

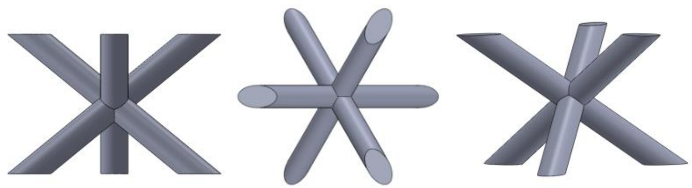

Front View Top view Perspective

Body centered (BC)

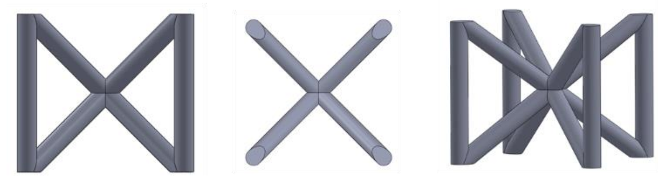

Front View Top view Perspective

Face centered (FC)

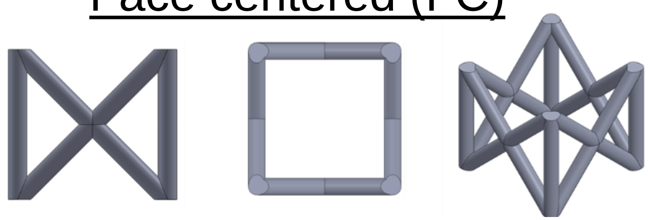

Front View Top view Perspective

Octahedral (Octa)

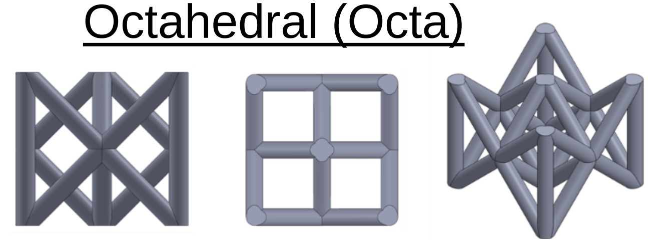

Front View Top view Perspective

Parameters	
Ligament diameter:	d
Unit cell base:	a
Unit cell height:	h
Porosity:	p
Total surface area:	A_{surf}
Footprint area:	A_{fp}
Orientation with flow:	θ

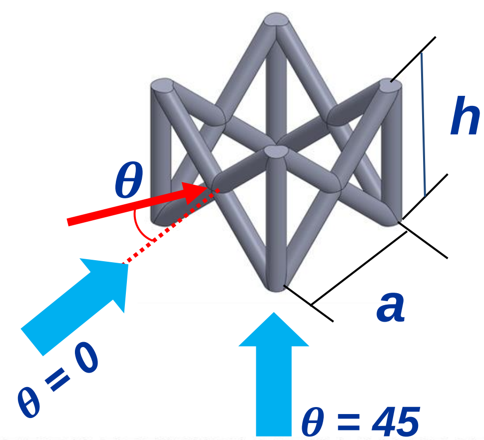

Scaled-Up Geometries

- 5x scaled up
- Inline arrangement of unit cells
- 0 and 45 degrees for cubic unit cells
- To study local distribution of the HTC on end walls

$$Porosity = 1 - \frac{solid\ volume}{total\ volume}$$

Geometry	Porosity
BC0 and BC45	0.77
FC0 and FC45	0.82
OCTA0 and OCTA45	0.65
Kagome	0.88
Pin bank	0.748

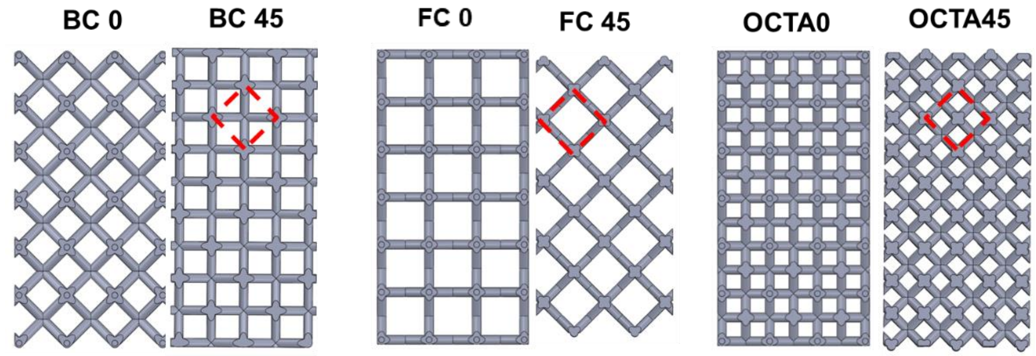

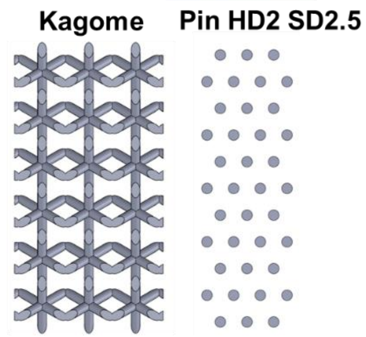

True scale unit cell
a = 4 mm
h = 2.54 mm
θ = 0 and 45 degrees
D = 0.75 mm

Scaled up (5x)
a = 20 mm
h = 12.7 mm
D = 3.75 mm

- Thermally inactive lattices
- Fabricated using SLA
- Nylon pin fins

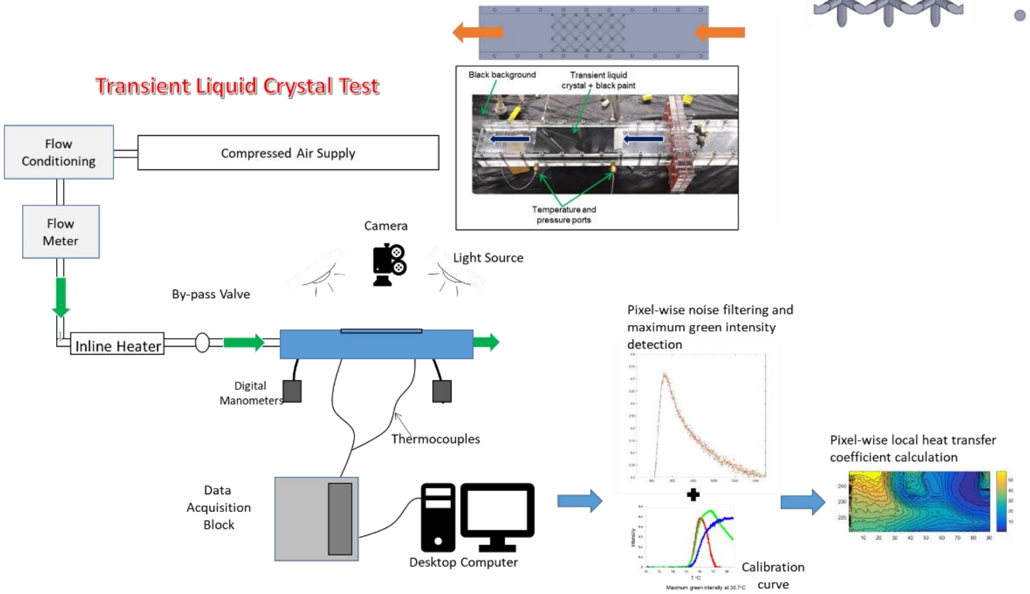

Transient liquid crystal test

- Step change in air temperature created
- Full color change history for each pixel monitored
- Noise filtering and peak detection algorithm for **maximum green component intensity** from RGB data

Summary of Transient Liquid Crystal Results

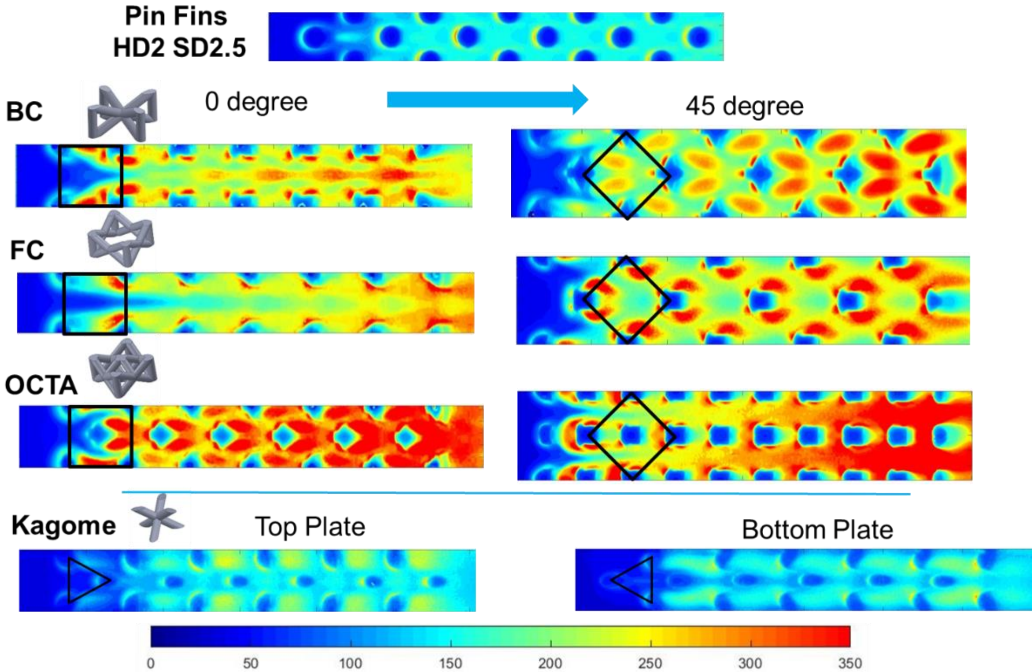

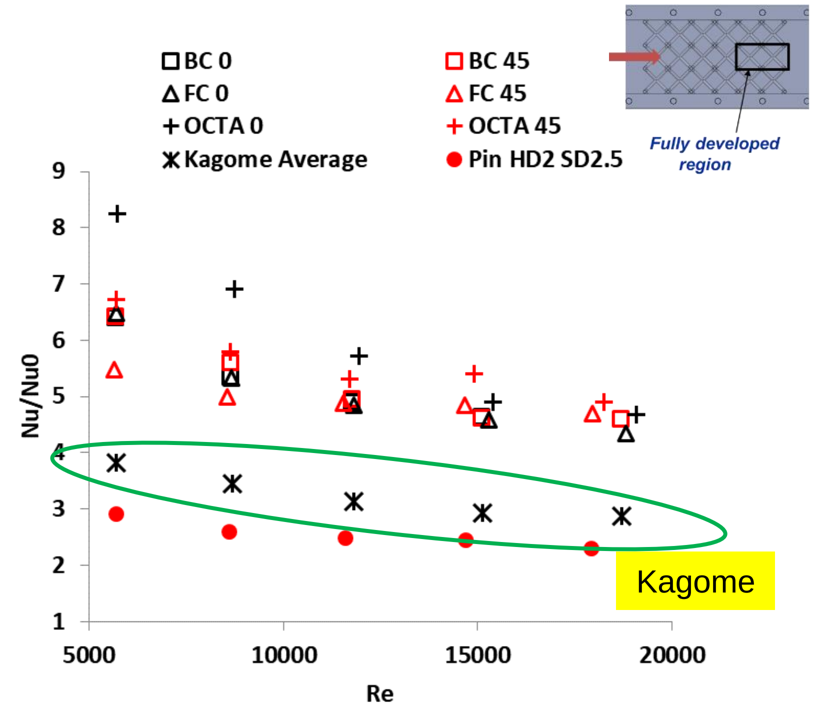

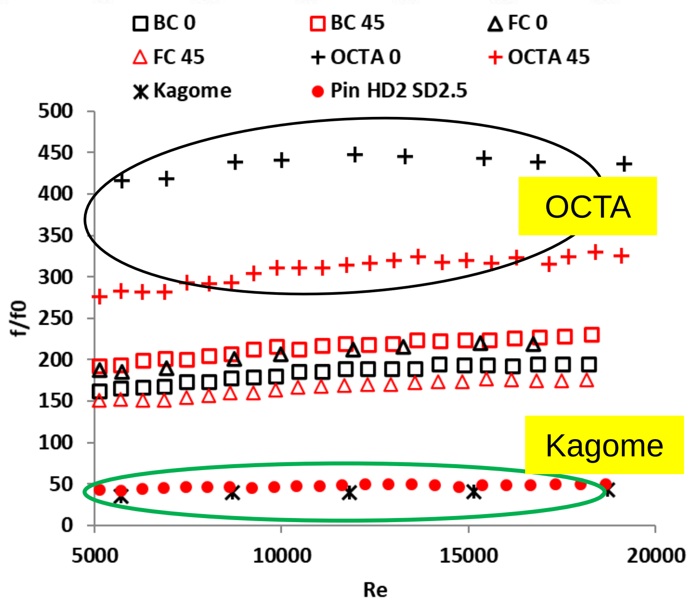

- Lattices provided higher heat transfer compared to that of the baseline pin-fin bank
- The unit cell geometry as well as their orientation w.r.t. flow affected the heat transfer and pressure drop behavior. However, the pressure drop characteristics had a stronger dependency on the unit cell rotation
- Asymmetrical HTC distribution in Kagome

Numerical Flow Field

- Steady State
- *Re_{ch}* : 11,700
- Convergence Criteria:
    - RMS Residuals = 10^{-5}
    - Imbalances = 0.1%
- *SST k-ω* turbulence model
- Ansys CFX

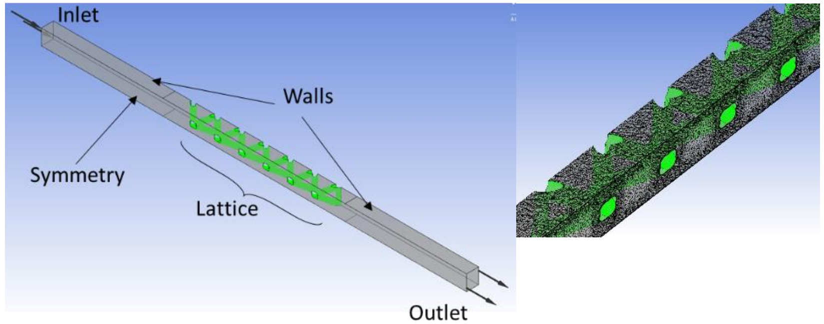

Comparison with experiment data

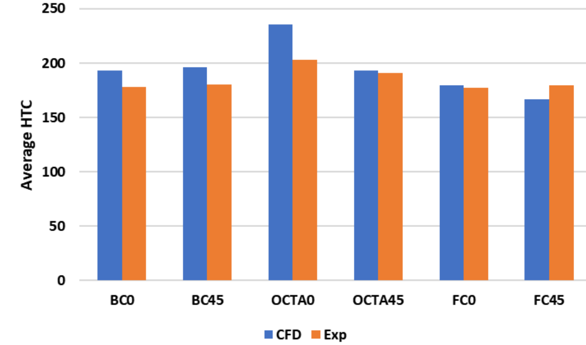

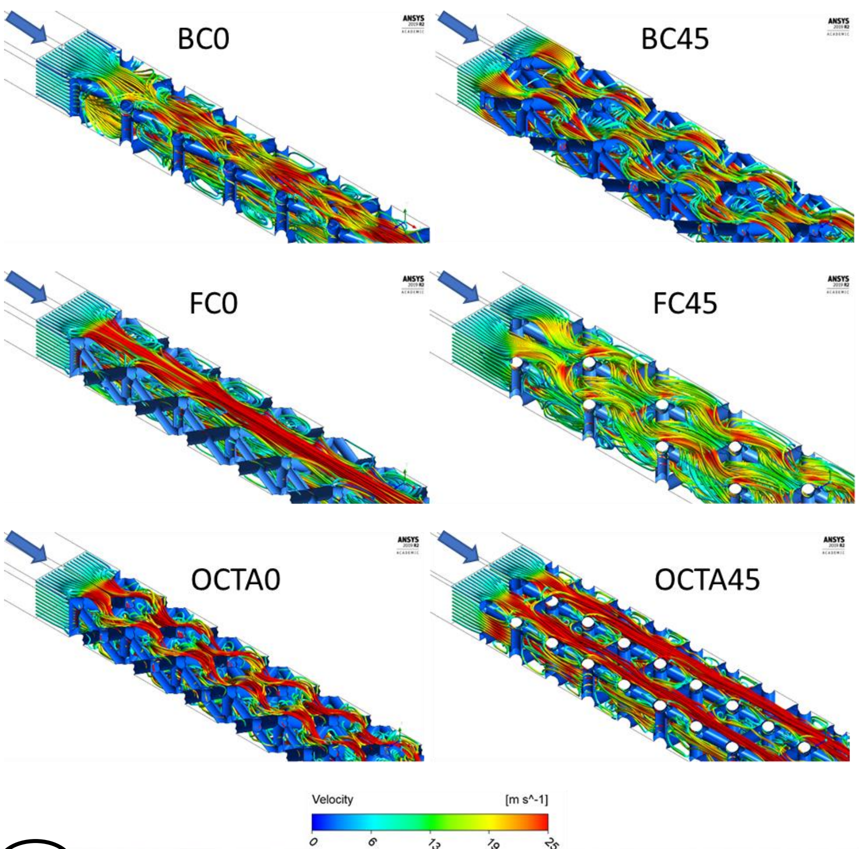

- ➢ Complex **subchannels** in cubic lattices
- ➢ Kagome produced **asymmetric** flow field
- ➢ Lattices provide opportunity to favorably redistribute coolant

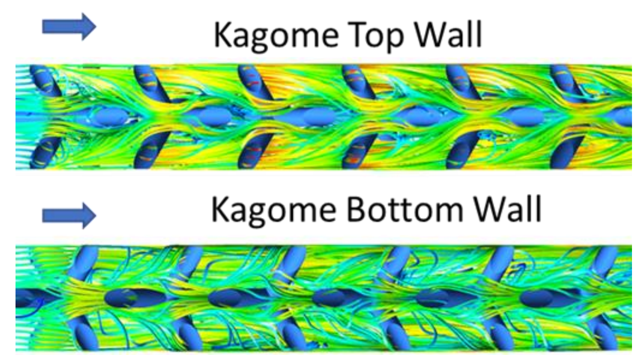

Entropy-Based Topology Optimization

Objective

- Identify high dissipation and low heat transfer regions within the flow
- Replace these regions with solid domain to:
  - (a) reduce dissipation, and
  - (b) increase heat transfer in dissipation dominated regions
- Entropy production rate per unit volume is ($Wm^{-3}K^{-1}$):

$$s_{tot} = s_h + s_f$$

(Bejan 1996), (Paoletti, Rispoli, and Sciubba 1989), (Kock and Herwig 2004), (Herwig and Kock 2006), (Herwig and Schmandt 2014)

Due to heat transfer

$$s_h = (\underbrace{s_{\bar{h}}}_{\text{Mean part}} + \underbrace{s_{h'}}_{\text{Turbulent part}})$$

$$s_{\bar{h}} = \frac{\lambda}{\bar{T}^2}\left[\left(\frac{\partial \bar{T}}{\partial x}\right)^2 + \left(\frac{\partial \bar{T}}{\partial y}\right)^2 + \left(\frac{\partial \bar{T}}{\partial z}\right)^2\right]$$

$$s_{h'} = \frac{\alpha_t}{\alpha} s_{\bar{h}}$$

μ = dynamic viscosity (kg/ms)
λ = thermal conductivity
α = molecular thermal diffusivity (m^2/s)
α_t = turbulent thermal diffusivity (m^2/s)
ϵ = specific dissipation of kinetic energy (m^2/s^3)

Due to friction losses

$$s_f = (\underbrace{s_{\bar{f}}}_{\text{Mean part}} + \underbrace{s_{f'}}_{\text{Turbulent part}})$$

$$s_{\bar{f}} = \frac{\mu}{\bar{T}}\left[2\left\{\left(\frac{\partial \bar{u}}{\partial x}\right)^2 + \left(\frac{\partial \bar{v}}{\partial y}\right)^2 + \left(\frac{\partial \bar{w}}{\partial z}\right)^2\right\} + \left(\frac{\partial \bar{u}}{\partial y} + \frac{\partial \bar{v}}{\partial x}\right)^2 + \left(\frac{\partial \bar{u}}{\partial z} + \frac{\partial \bar{w}}{\partial x}\right)^2 + \left(\frac{\partial \bar{v}}{\partial z} + \frac{\partial \bar{w}}{\partial y}\right)^2\right]$$

$$s_{f'} = \frac{\rho\epsilon}{\bar{T}}$$

- For a given volume, total entropy generation (WK^{-1}) is:

$$S_f = \int s_f \, dV \qquad S_h = \int s_h \, dV$$

$$S_{tot} = S_h + S_f$$

- Defining Bejan number (Be) as: $Be = \dfrac{S_h}{S_{tot}}$

All variables readily available in a steady state numerical solution

Optimization Process

Overview of the topology optimization process

Steady State Conjugate CFD
↓
Calculate Entropy Rates
↓
Filter Low Be Regions
↓
Replace with Solid Domain

Features
- Single iteration process
- No custom solver needed, can be implemented as a post process
- Optimizes preexisting topology

Application to BC0 unit cell

- ➢ Conjugate problem with both solid and fluid domains
- ➢ Only half domains used due to symmetry
- ➢ Boundary conditions based on TLC experiment data

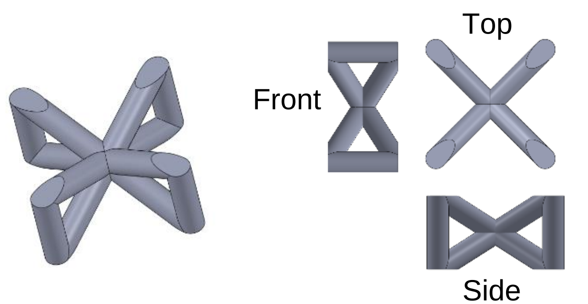

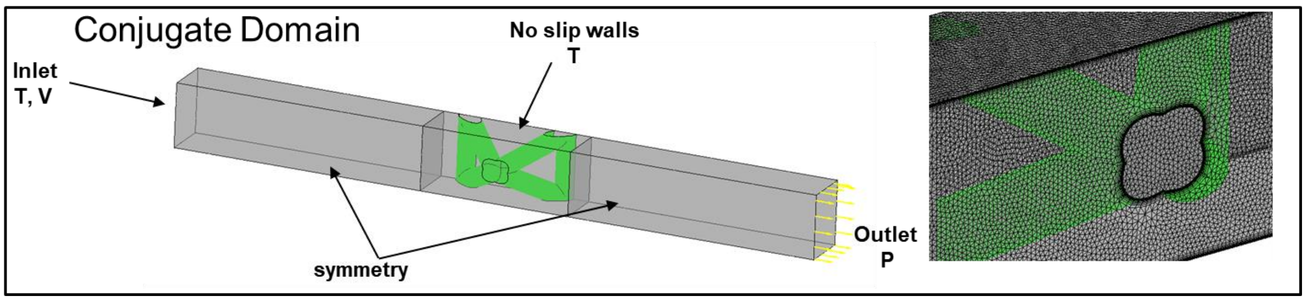

CFD setup
- Re_{ch} : 11,700
- Convergence Criteria:
  - RMS Residuals = 10^{-5}
  - Imbalances = 0.1%
- *SST k-ω* turbulence model
- Ansys CFX

Entropy Generation with Be

- To facilitate optimization of geometry, the entropy generation analysis was confined to fluid regions with **u**<=0, comprised mostly of lattice wake regions
- As shown in cumulative plot, such regions accounted for up to 11.8% of channel fluid volume, 18.3% of channel S_f, and 20.9% of channel S_h

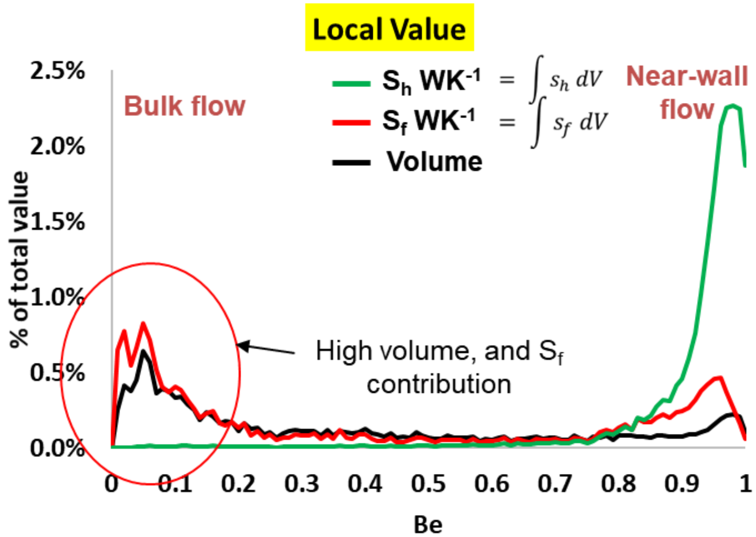

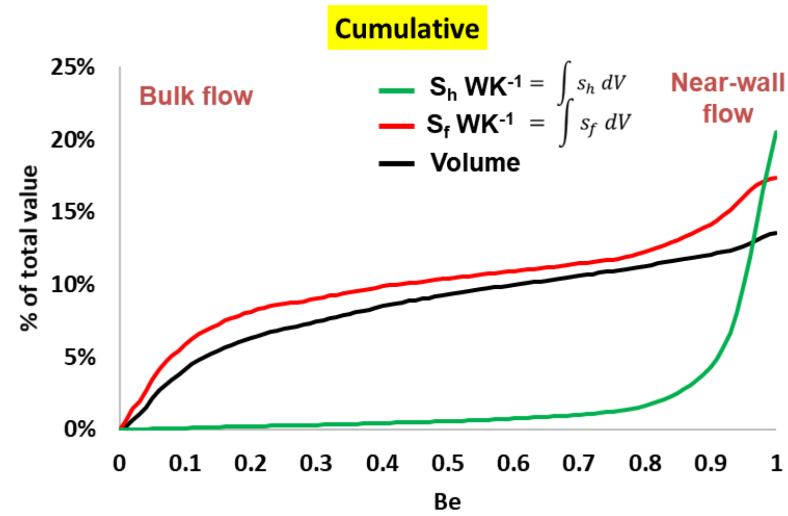

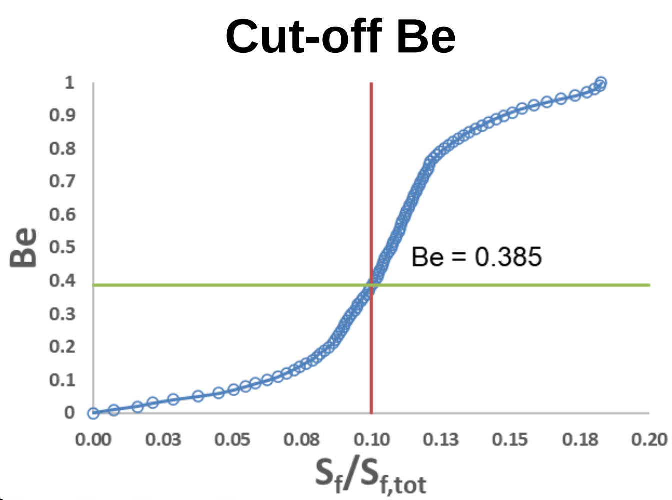

- Fix $S_f/S_{f,\,tot}$ ratio (here, 0.1)
- Calculate the corresponding Be
- Wake regions (**u**<=0) with Be lower than the cut-off value are of interest

Optimizing Low Be Regions (BC0)

- Instead of selecting all regions below cut-off Be, additional criteria of **u** <= 0 applied to filter connected fluid regions

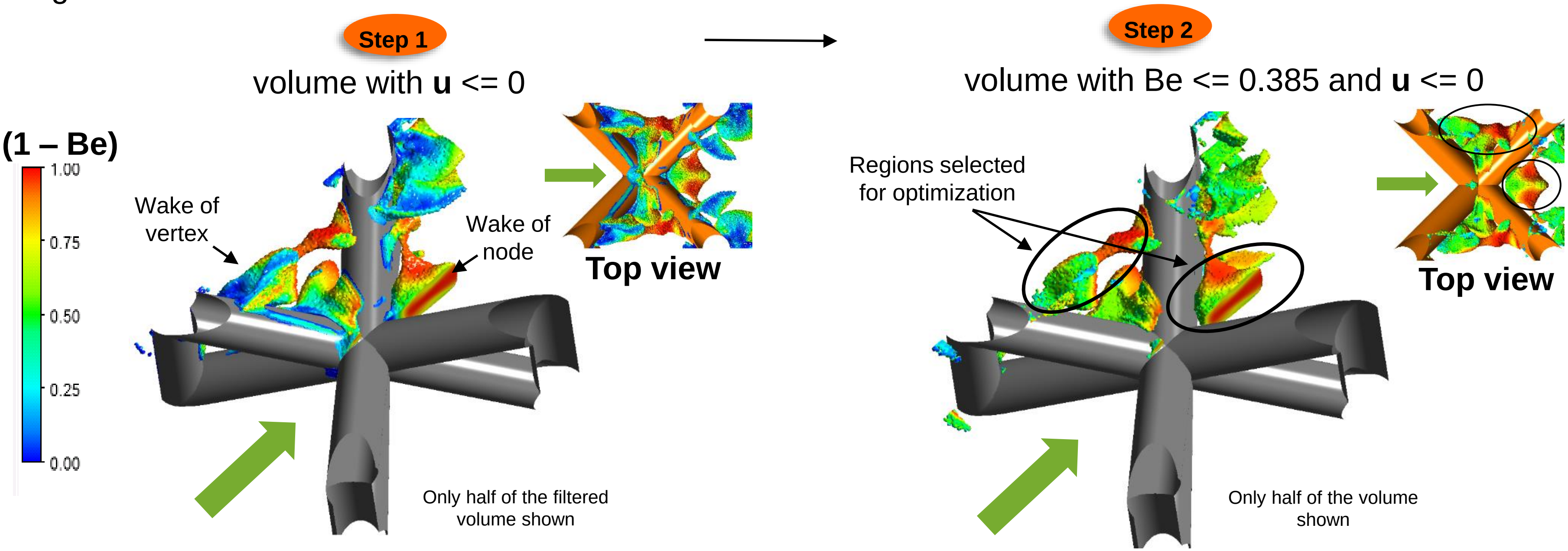

- Point cloud from filtered volume exported to CAD application and replaced with solid

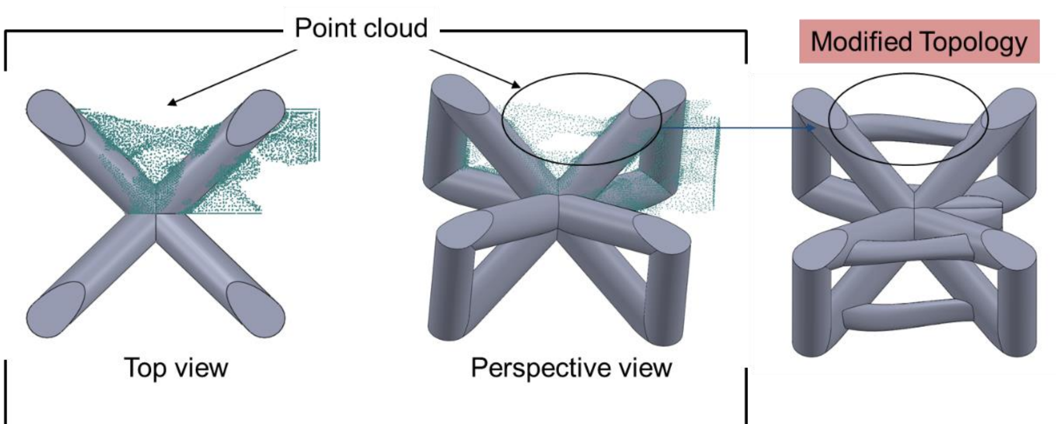

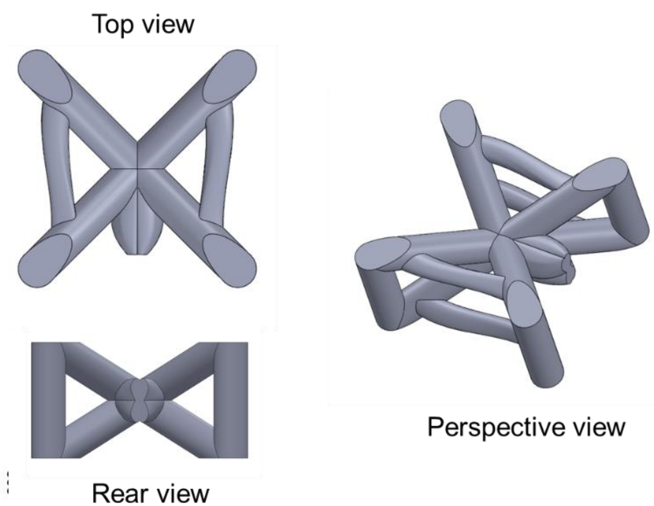

Result Summary

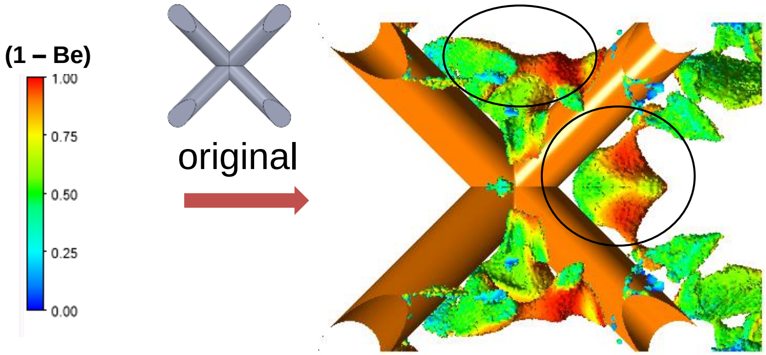

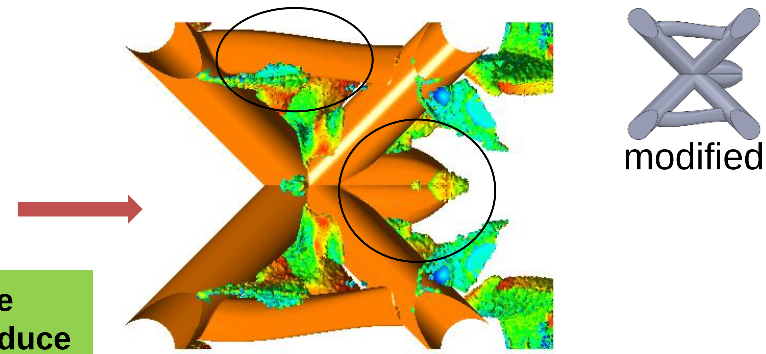

Low Be regions reduce by ~40%.

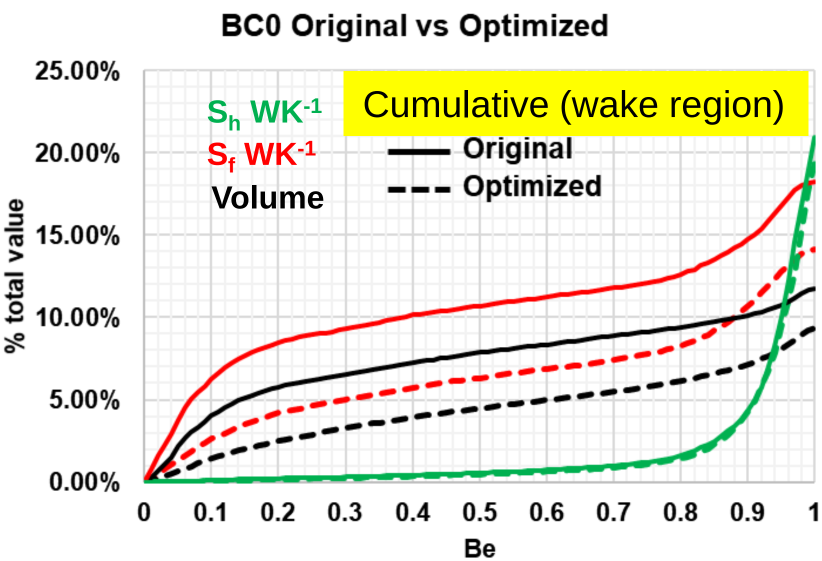

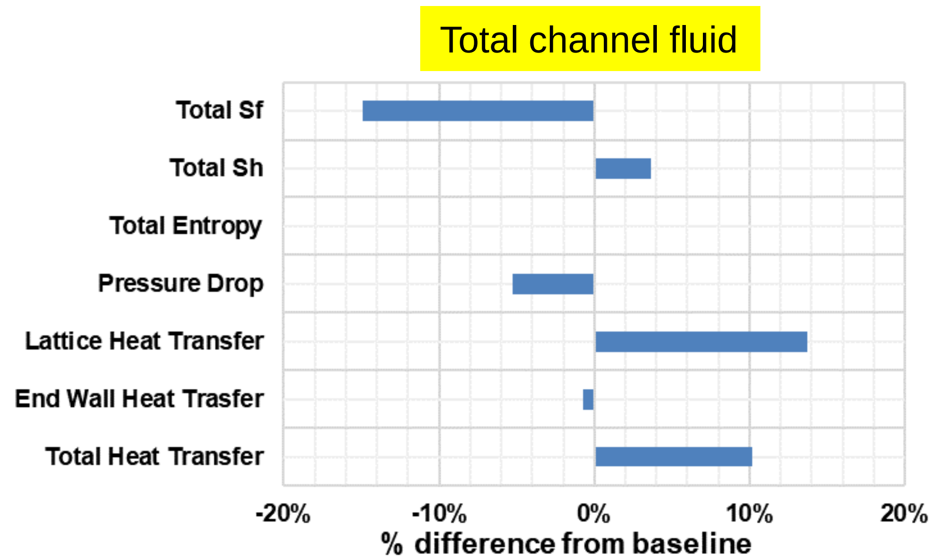

- S_f decreased at each Be level within wake regions (**u** <= 0)
- Relatively small change in S_h, indicating heat transfer preserved

- S_h increased while S_f decreased
- Reduction in S_f improved pressure loss
- The overall heat transfer improved due to added conduction pathway

The method facilitates strategic modification of geometry to improve aero-thermal performance

Experimental Result for Pressure Drop

- Optimized unit cell was arranged to obtain a lattice and printed

CAD model

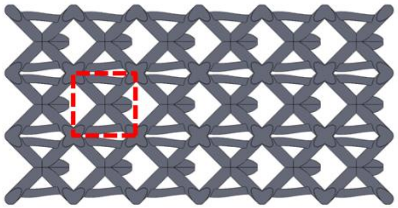

Printed lattice

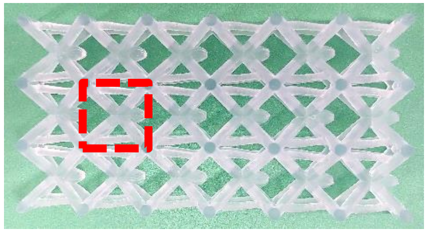

Geometry	Surface Area (m²)	Volume (m³)	Porosity
BC0	2.16E-02	2.30E-05	0.77
BC45	2.45E-02	2.64E-05	0.75
BC0 Optimized	2.67E-02 ↑	2.72E-05	0.73 ↑

Pressure drop comparison

$$f = \frac{\left(\frac{\Delta p}{\Delta x}\right) D_{ch}}{\frac{\rho U^2}{2}}$$

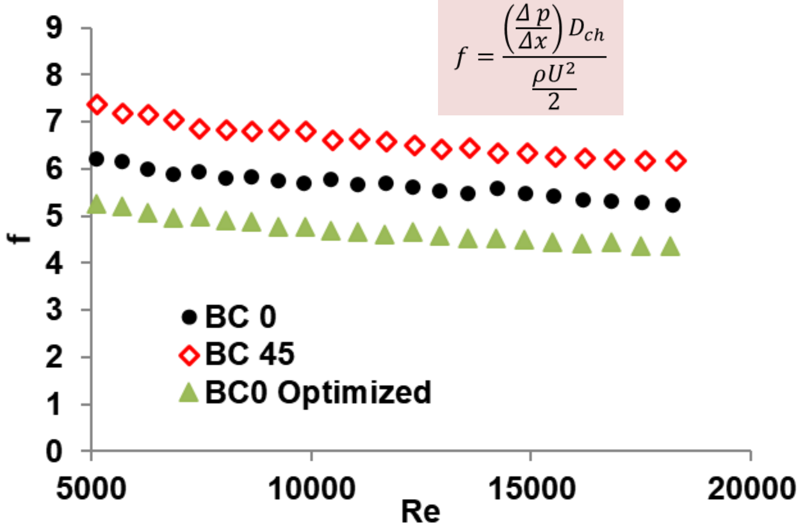

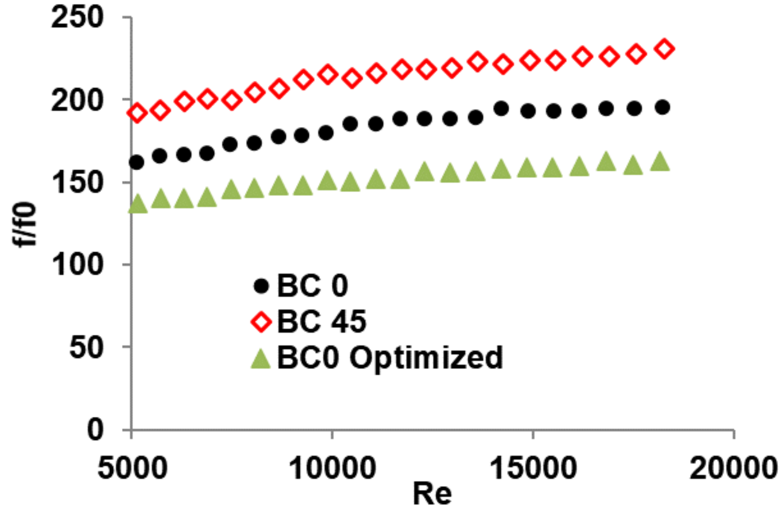

- Despite increase in surface area and decrease in porosity, ~15.6% decrease in pressure drop

Application to Other Unit Cells

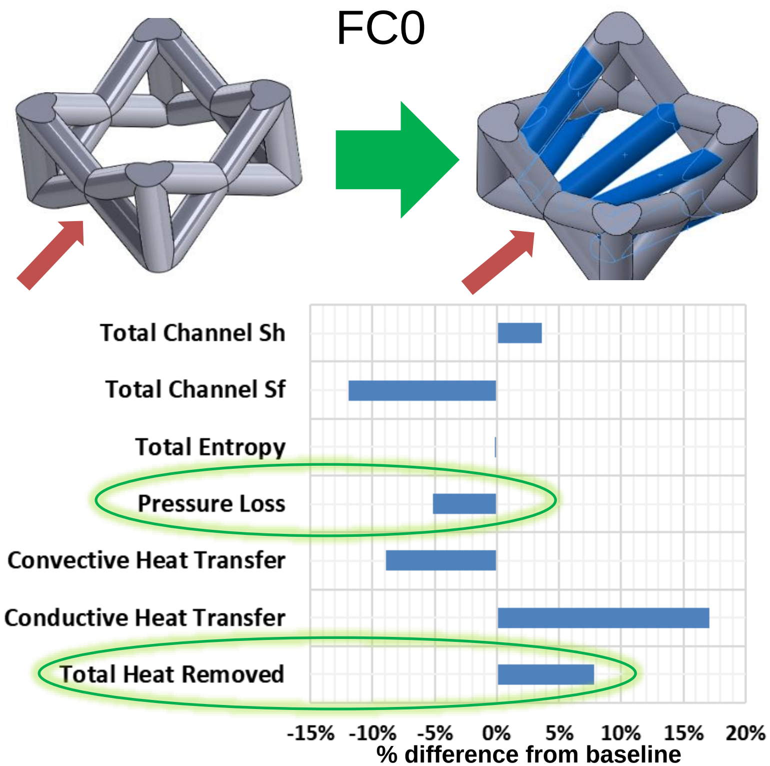

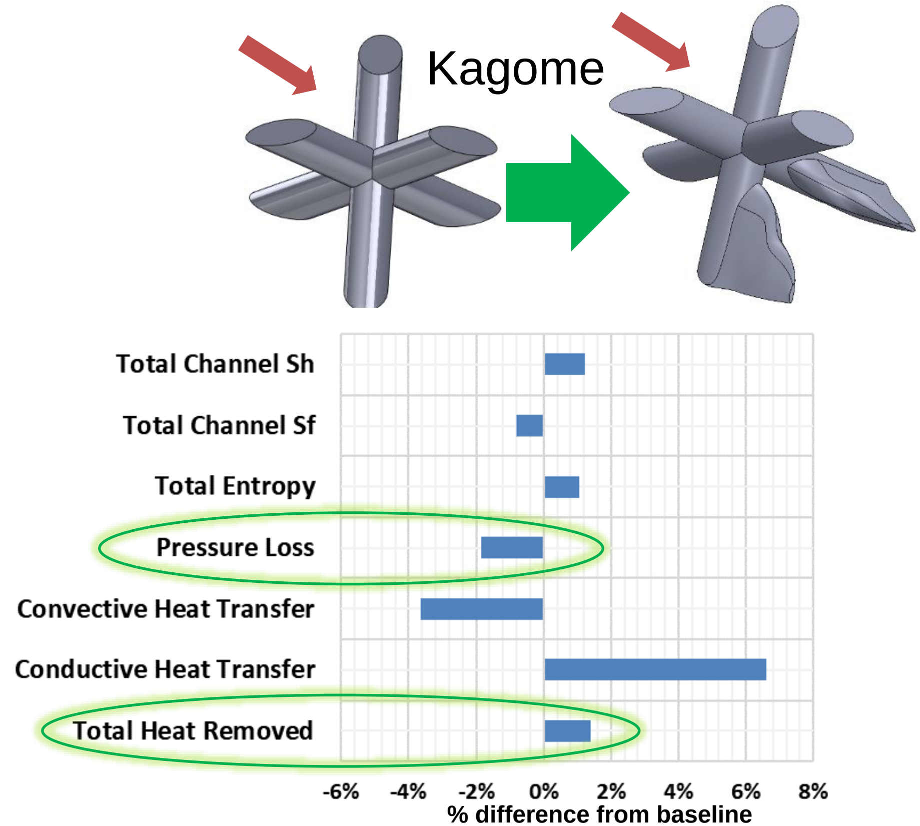

- Once again, improvement is observed in total heat removed and pressure drop

Integrated Cooling with Micro Scale Lattice (Phase 2)

- Transpiration for outer cooling, lattice for internal cooling
- Two possible designs based on coolant flow direction
- Testing will be carried out in the already stablished wind tunnel

Plenum-fed

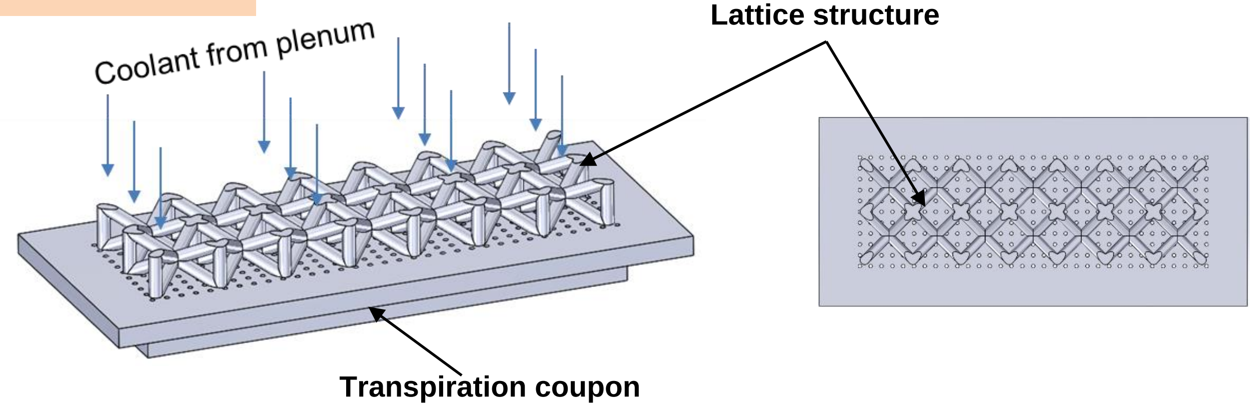

Plenum-fed geometries printed using DMLS

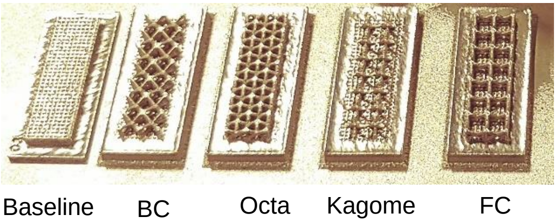

Crossflow-fed

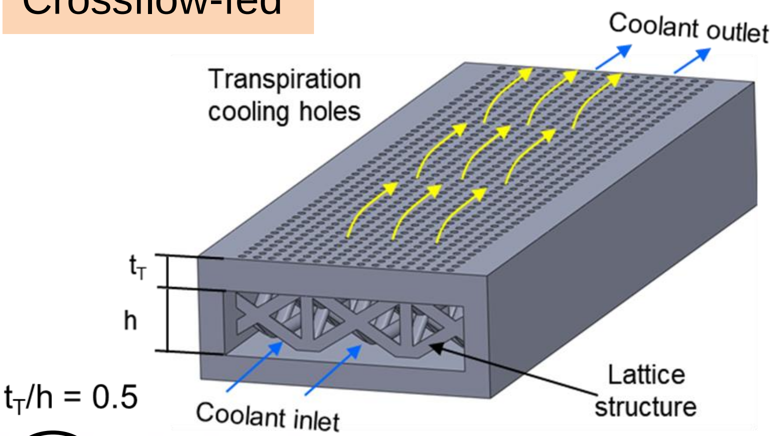

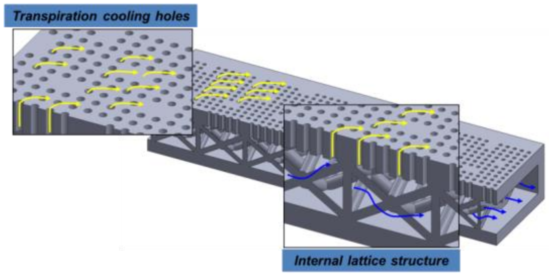

Crossflow-fed geometry printed using DMLS

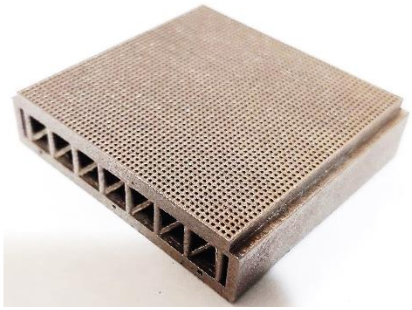

Summary of Heat Transfer Tasks

❑ Transpiration cooling

- The micro-lithography technique was employed to fabricate the surface heater on transpiration cooling target surface
- The adiabatic cooling effectiveness and HTC for the transpiration cooling structures were investigated for the first time
- Transpiration cooling with low blowing ratio (0.125) has higher adiabatic cooling effectiveness than multi-row film cooling and HTC ratio close to 1
- Although higher blowing ratio increases HTC significantly, the adiabatic cooling effectiveness of transpiration cooling is still higher than film cooling

❑ Lattice cooling

- Lattices are capable of providing high heat transfer
- Both geometry and orientation affects the local heat transfer on end walls
- New topology optimization method based on second law analysis was introduced and demonstrated to improve heat transfer and pressure drop in lattices
- Two possible integrated design based on coolant flow direction being investigated

Outlines

- *Background, Challenges, Objectives, Benefits of Technology, Research Task Plans*
- *Additive Manufacturing Processes*
- *Heat Transfer Results: Transpiration Cooling*
- *Heat Transfer Results: Lattice Cooling*
- ***ODS Powder Development***
- *Summary*

Ni- and Fe-based ODS powder development for Additive Manufacturing of gas turbine component with better high temperature (up to 1200 ^{o}C) oxidation/corrosion resistance and material strength (i.e. creep and fatigue)

(i) (to produce) ODS powder for AM with lower manufacturing cost and better yttria dispersion using a combined Hosokawa mechano chemical bonding (MCB) and ball milling (BM) process:

(a) MCB + BM

(b) MCB only

(ii) AM processing optimization

(iii) (to achieve) a durable α-Al_2O_3 oxide layer with strong adhesion to substrate (via external oxidation) for better oxidation and corrosion resistance

Nickel-based ODS alloys fabricated by AM

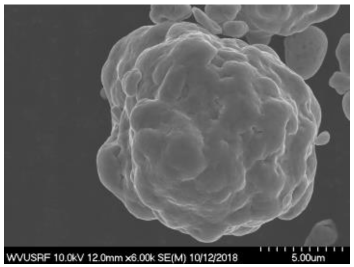

Oxide layer

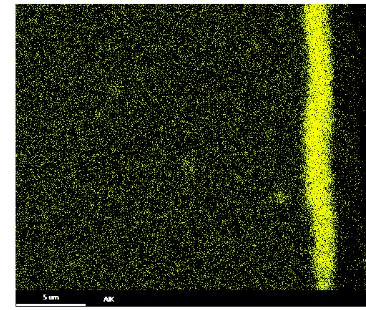

Powder + AM → ODS

Microstructure

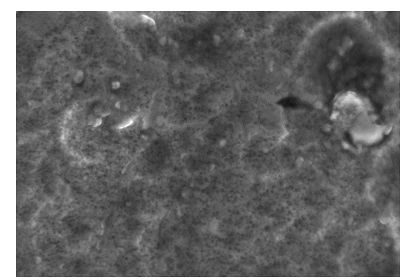

ASME Allowable Stress for High Temperature Alloys

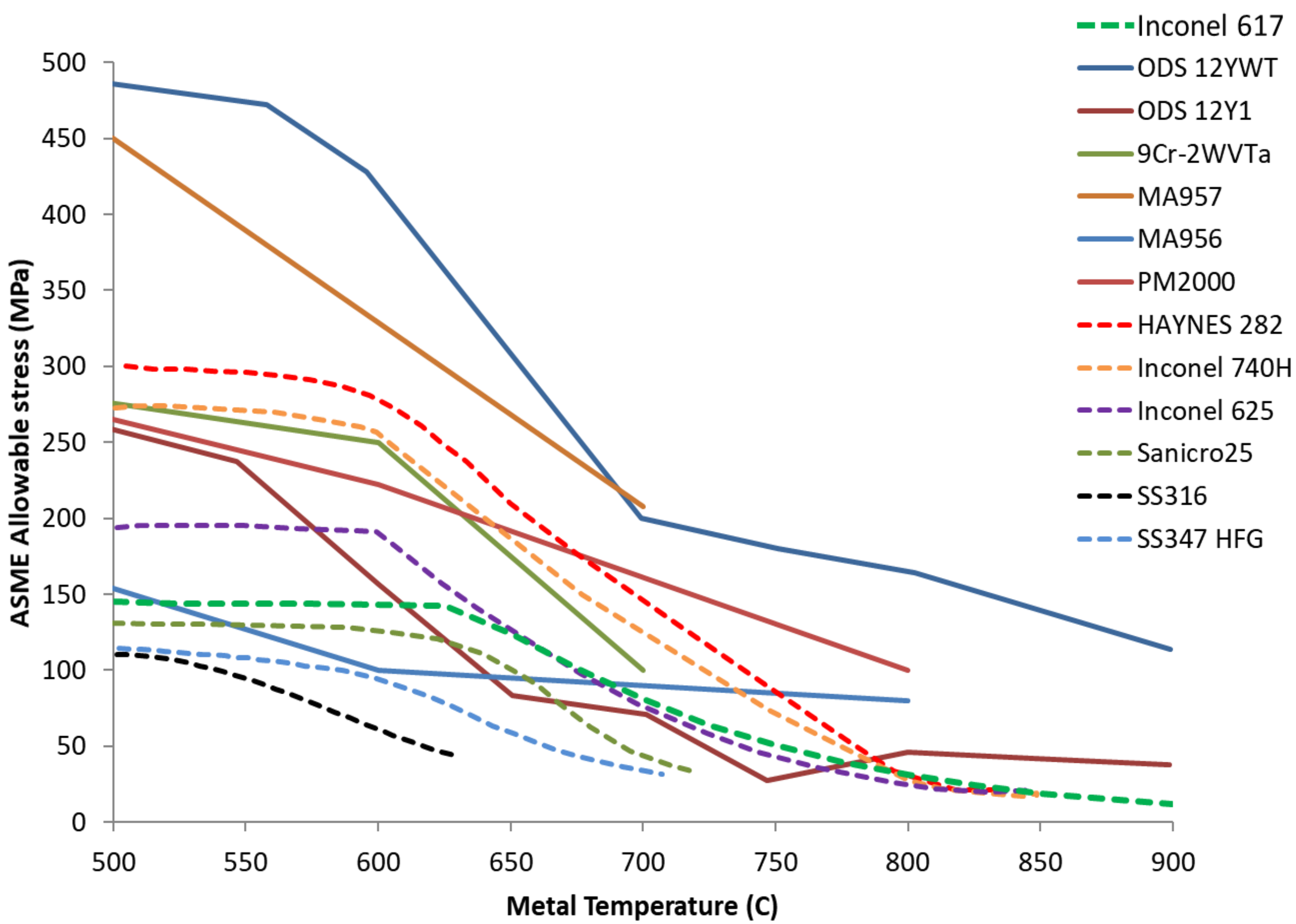

ODS Powder Compositions (in weight %)

	Cr (7.5~10 µm)	Al (4.5 ~ 7 µm)	Y_2O_3 < 50nm	W (~1 µm)	Ni (4 ~ 8 µm)
A1	20	5	1.5	0	73.5
A2	20	5	1.5	3	70.5

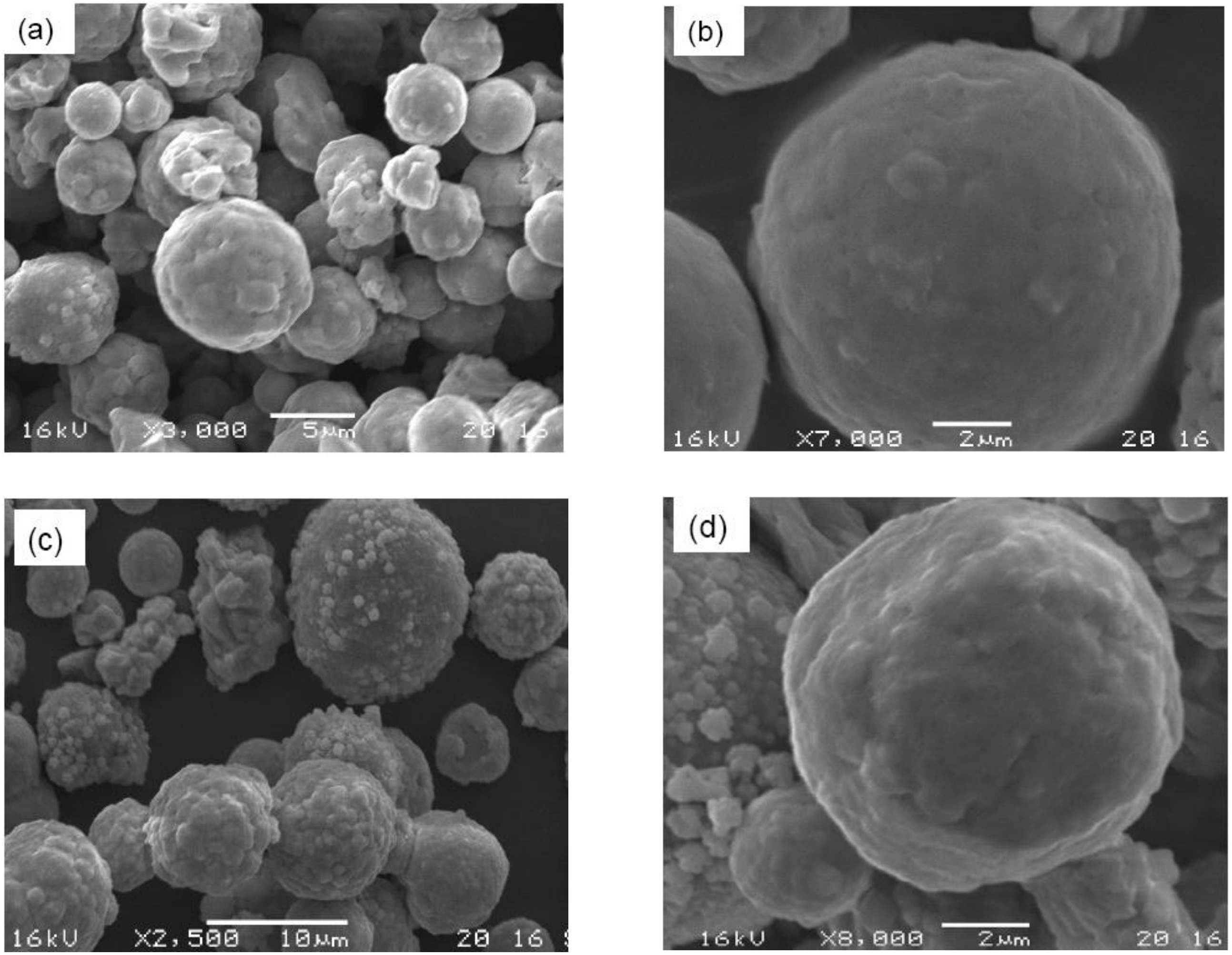

SEM micrographs of MCB processed powder sample A1 and A2
(a). Sample A1; (b) close view of (a); (c) sample A2; (d): close view of (c)

ODS Powder Characterization

TEM BF and HREM imaging – A1 Sample

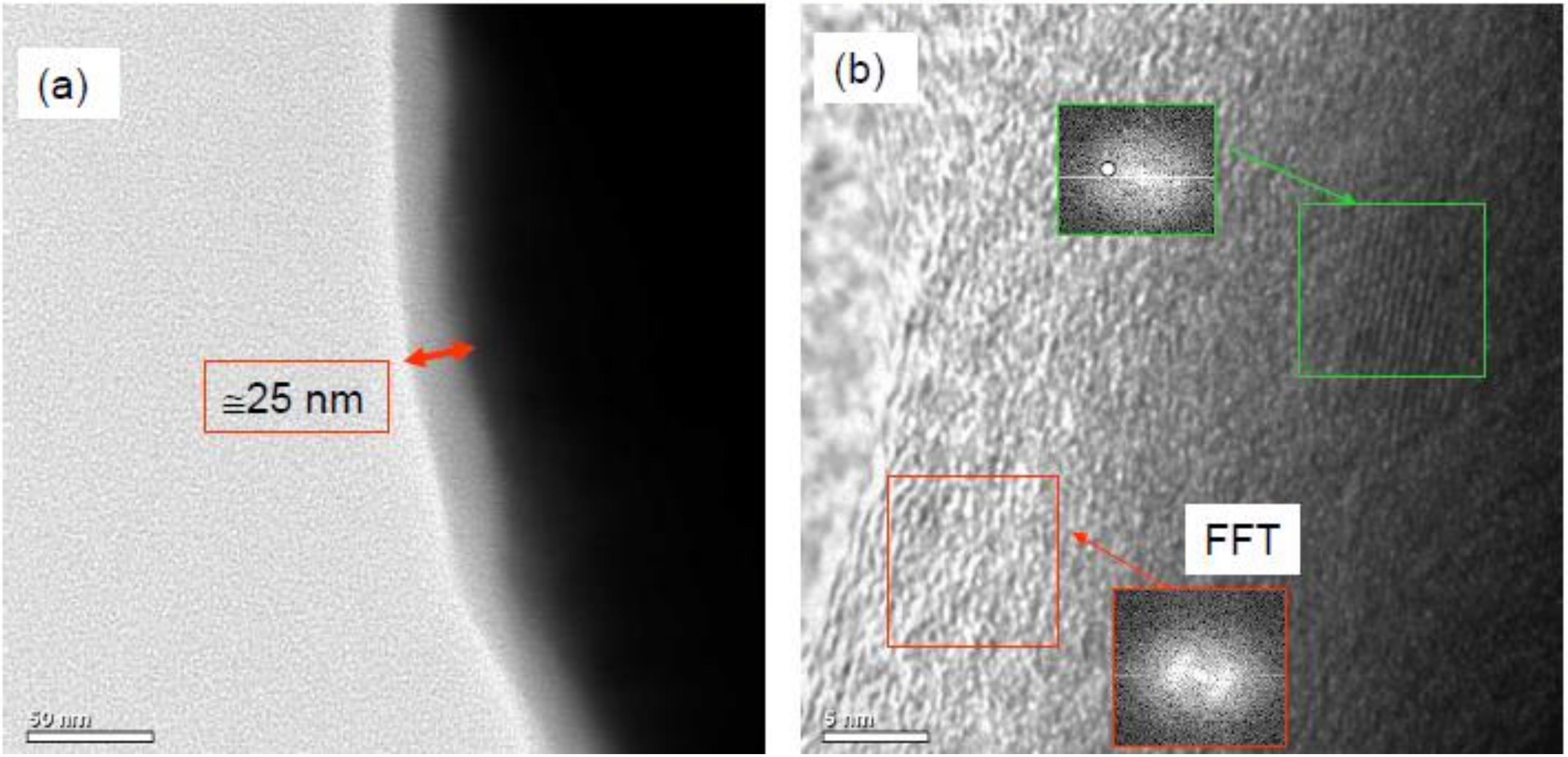

- TEM BF image (a) shows a layer of Y_2O_3 thin film with thickness about 25nm around the edge of particle. The film thickness is relatively homogeneous.
- HREM image (b) shows the fine structure of the thin film. Most area of the film is amorphous and the corresponding FFT (Fast Fourier Transform) image show the diffusive feature.
- There is crystal structure within film as FFT indicated. The embedded FFT shows the spots and image shows the orientation fringe. The growth of film may involve crystallization of Y_2O_3.

Y_2O_3 uniform dispersion by MCB

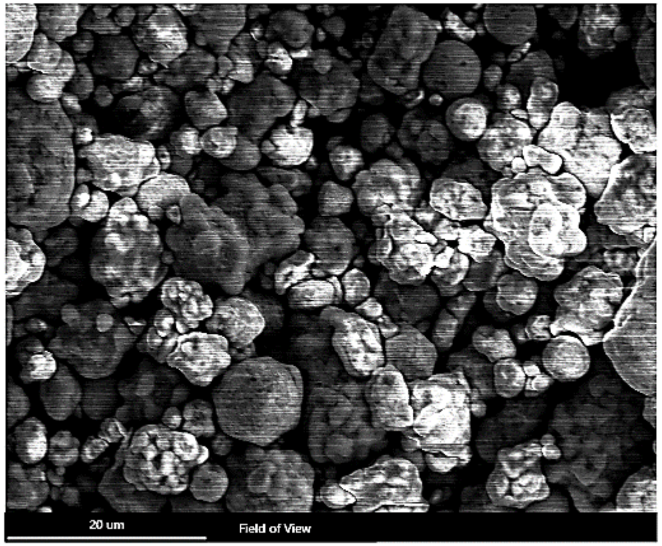

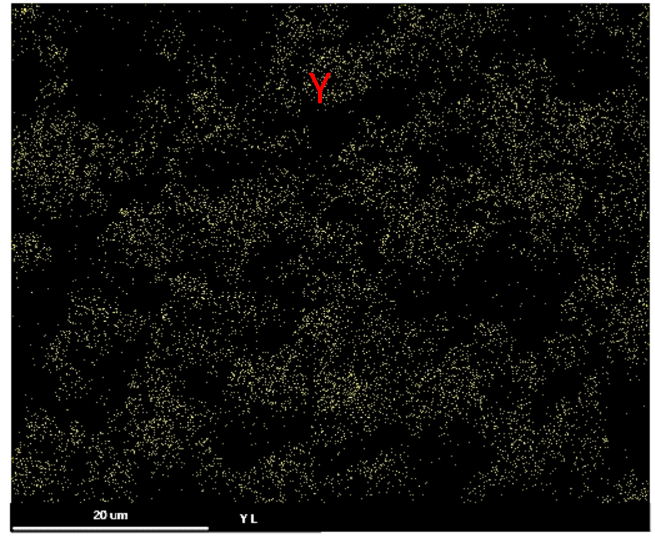

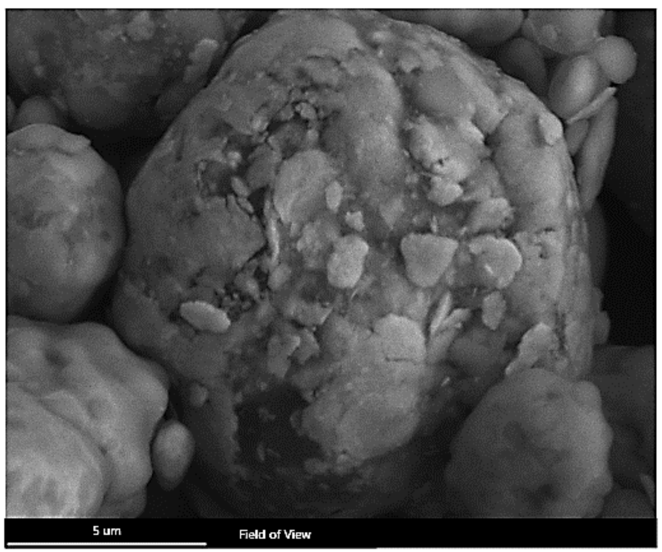

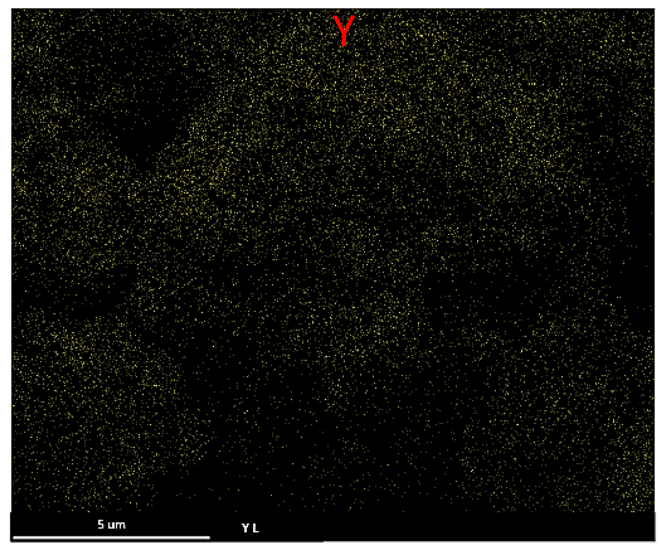

ODS Powder Characterization

MCB can break Y2O3 down and distribute Y2O3 uniformly in powders.

NiAl phase peak can be detected by XRD.

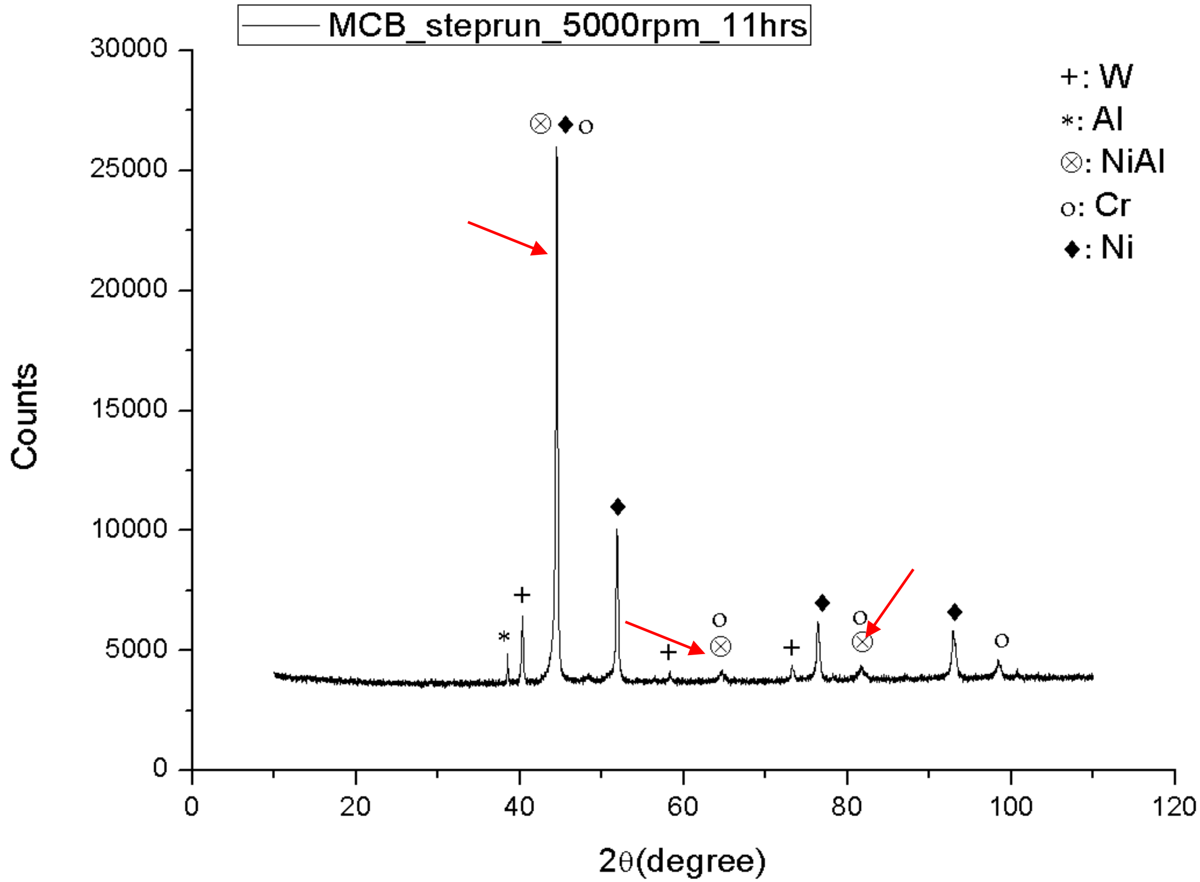

XRD spectrum of MCB-steprun-5000rpm-11 hours ODS powders ODS powders

Size Distribution

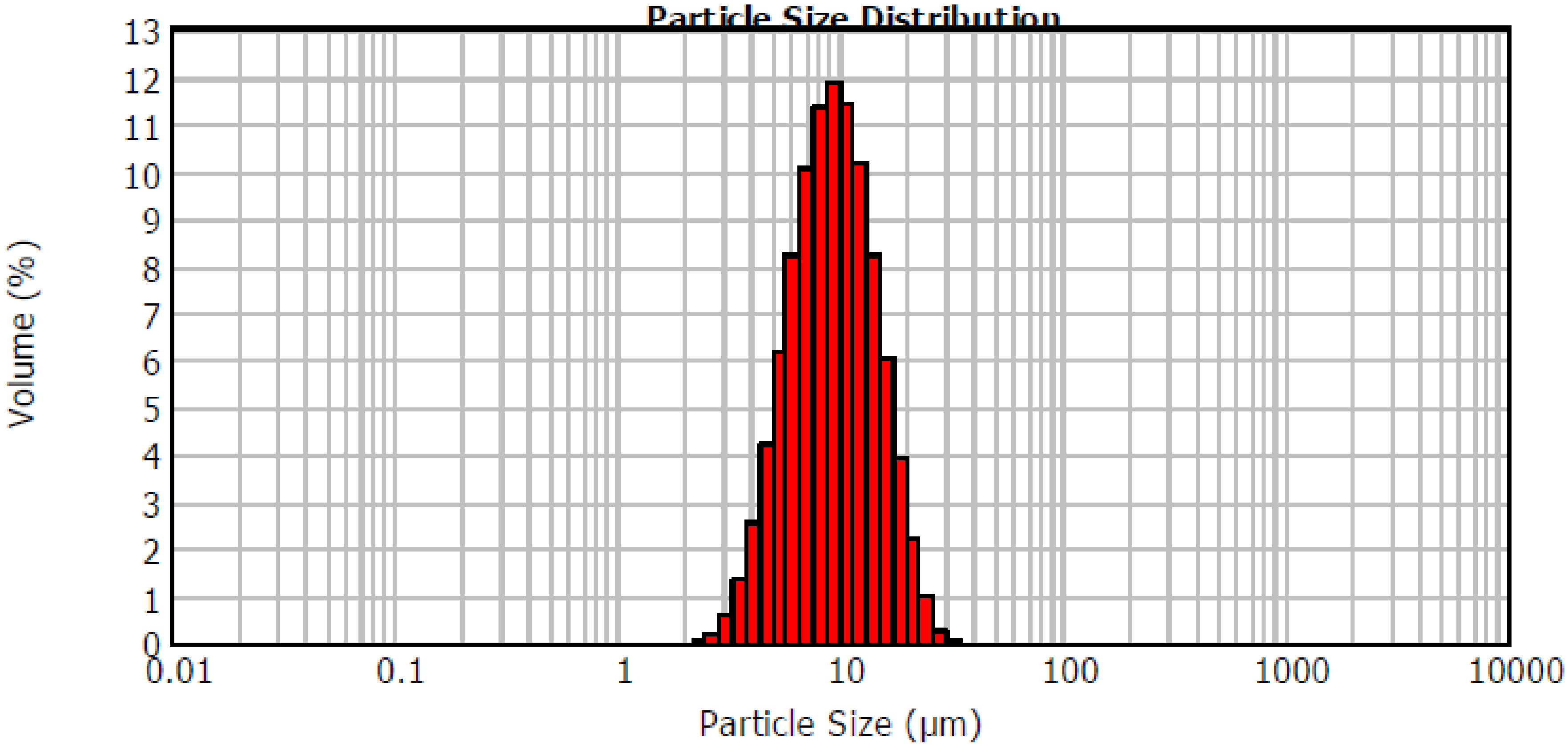

D(0.1)=5.153μm, D(0.5)=9.261μm, D(0.9)=16.296μm

200W ODS – AM Printed

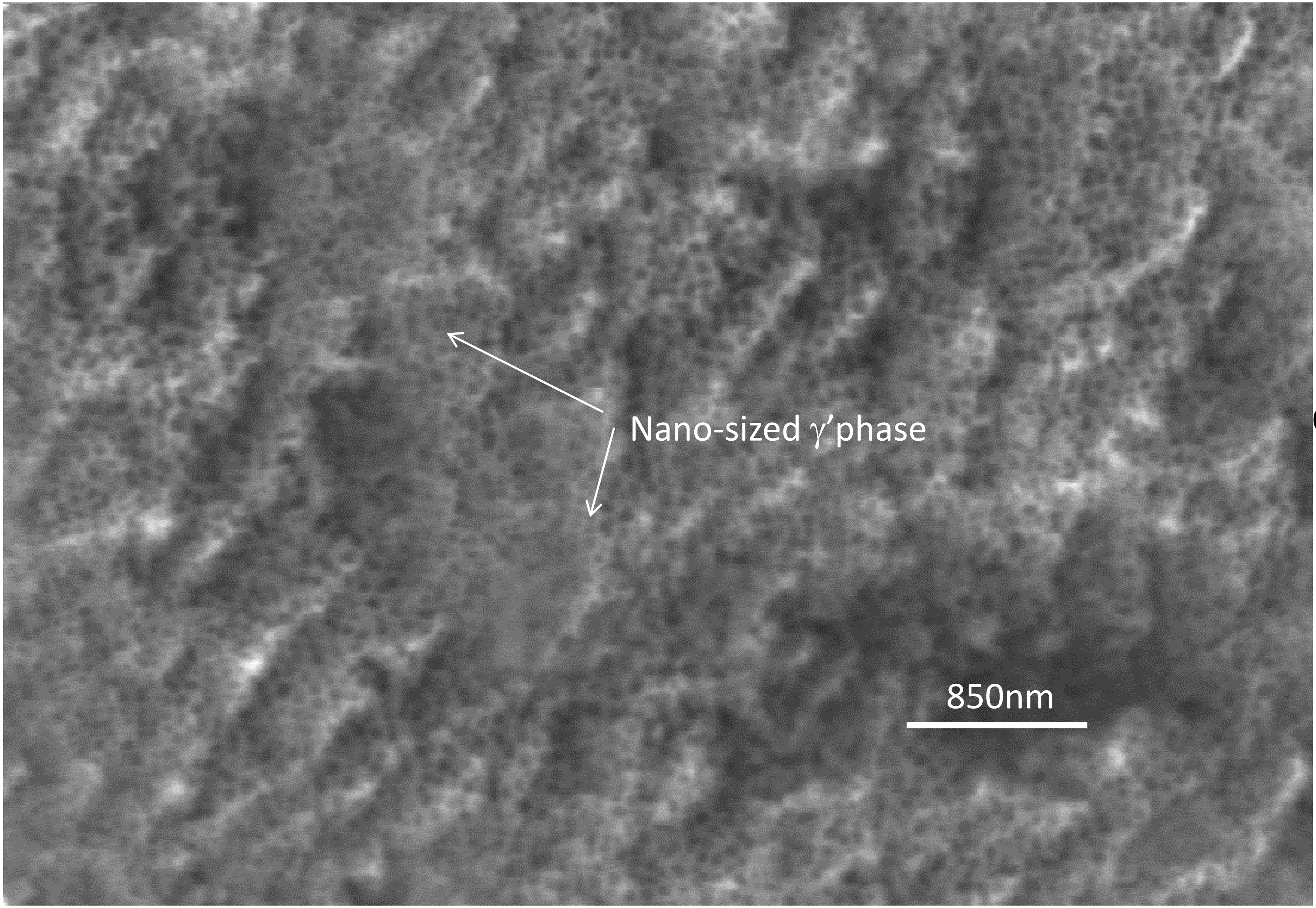

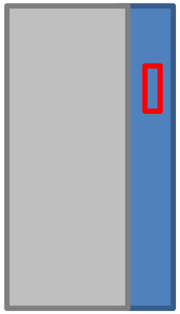

ODS Coating

200W ODS – 2200cycles

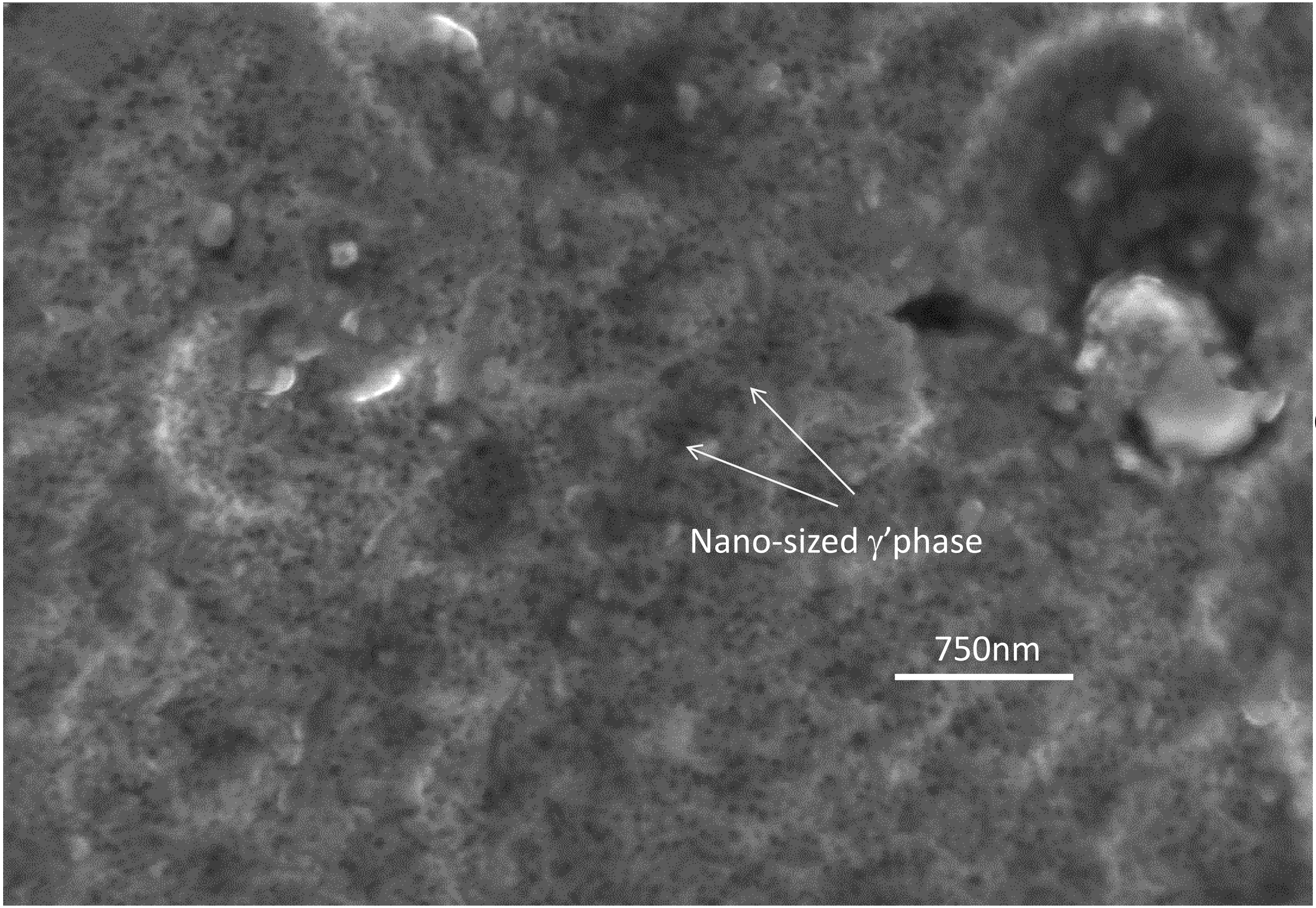

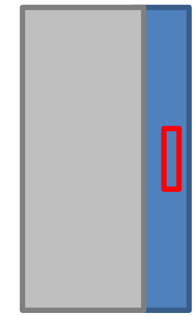

Nano-sized γ’phase preserved at ODS costing after 2200 cycles

γ’ phase in 200W ODS Coating
(DED AM)

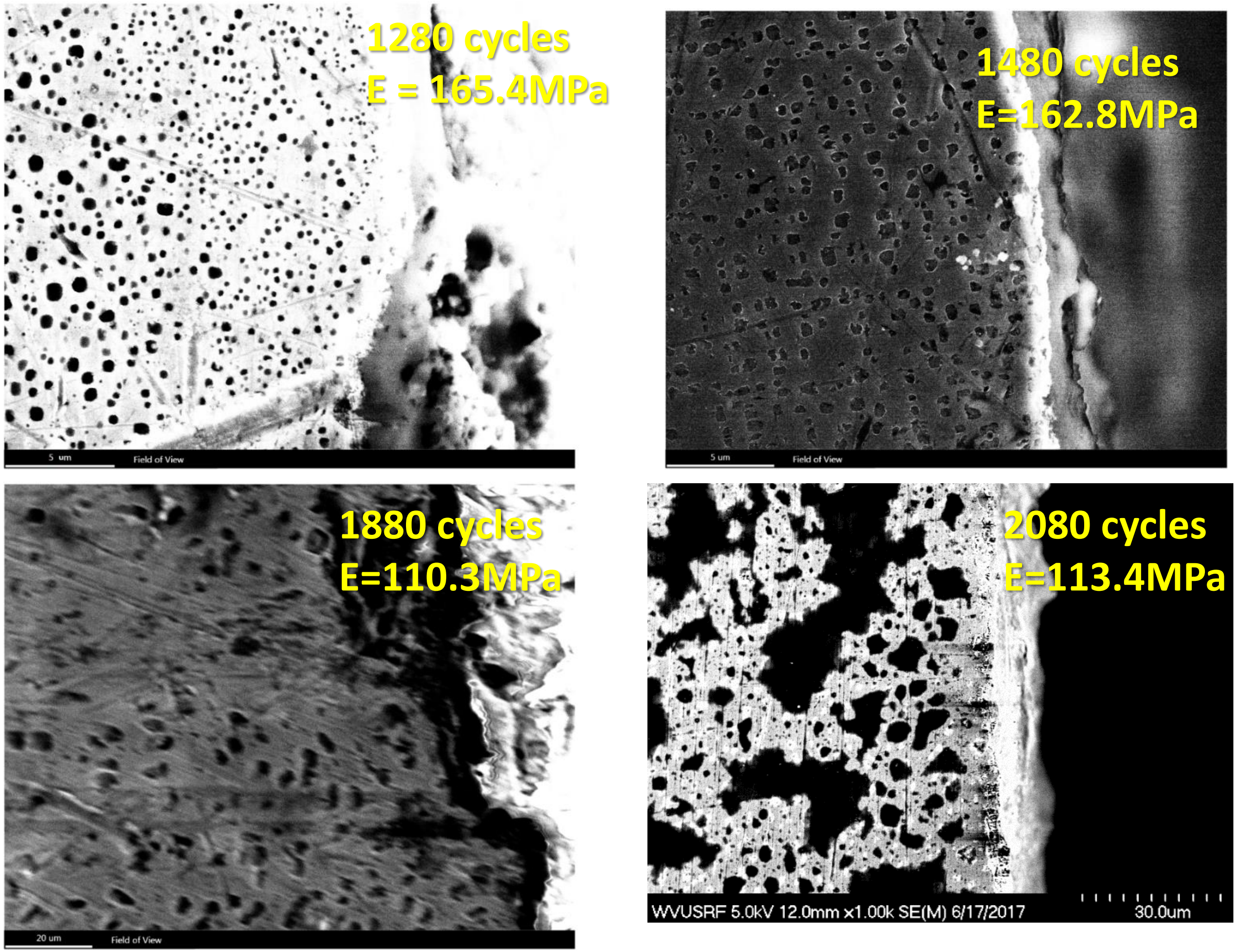

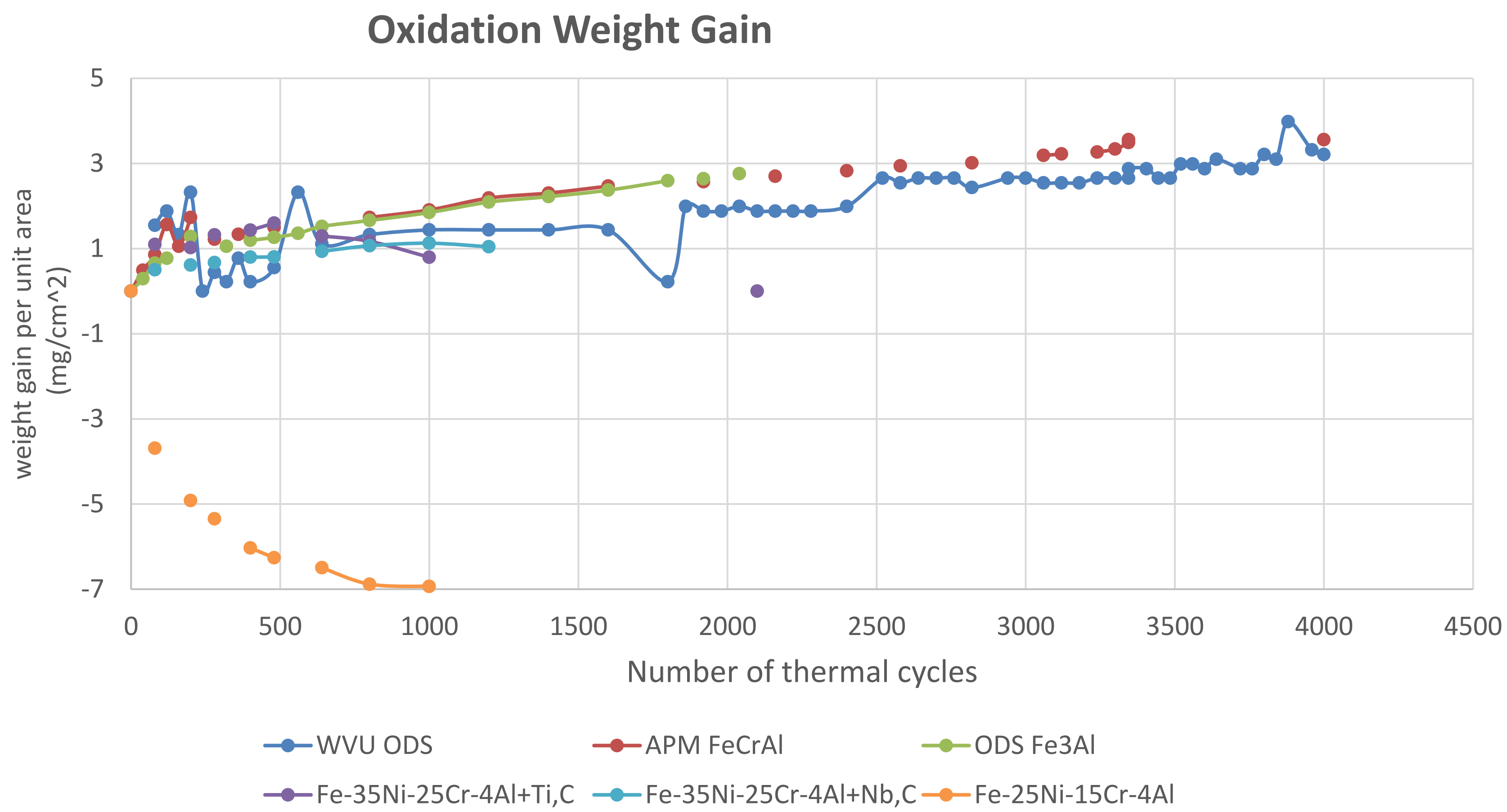

[1] Wright, I.G., Pint, B.A. & Tortorelli, P.F. Oxidation of Metals (2001) 55: 333. https://doi.org/10.1023/A:1010316428752
[2] Brady, M.P., Muralidharan, G., Yamamoto, Y. et al. Oxid Met (2017) 87: 1. https://doi.org/10.1007/s11085-016-9667-3

Comparison of oxidation weight gain of WVU ODS with other alumina forming alloys [1.2]

Oxide layer Stability Analyses of AM-processed ODS using LENS

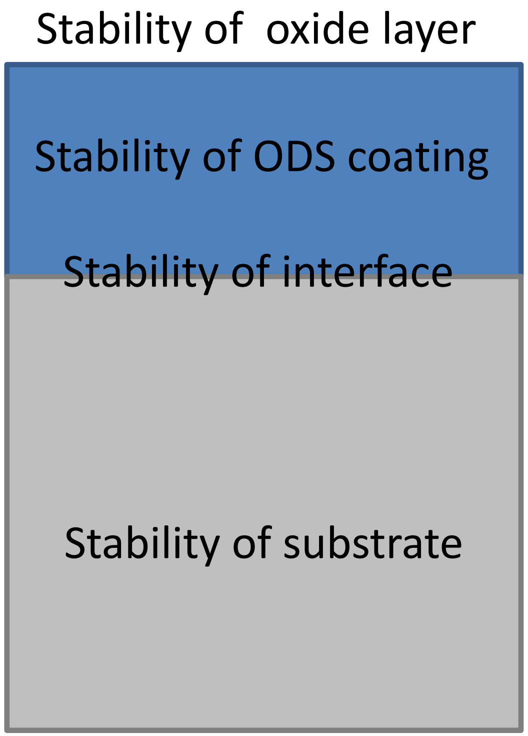

Uniform Distribution of Yttrium in As-printed ODS Sample

250W (BM+MCB) ODS, Scanning Speed 0.5 in/s,100 W In-situ Laser Heat Treatment

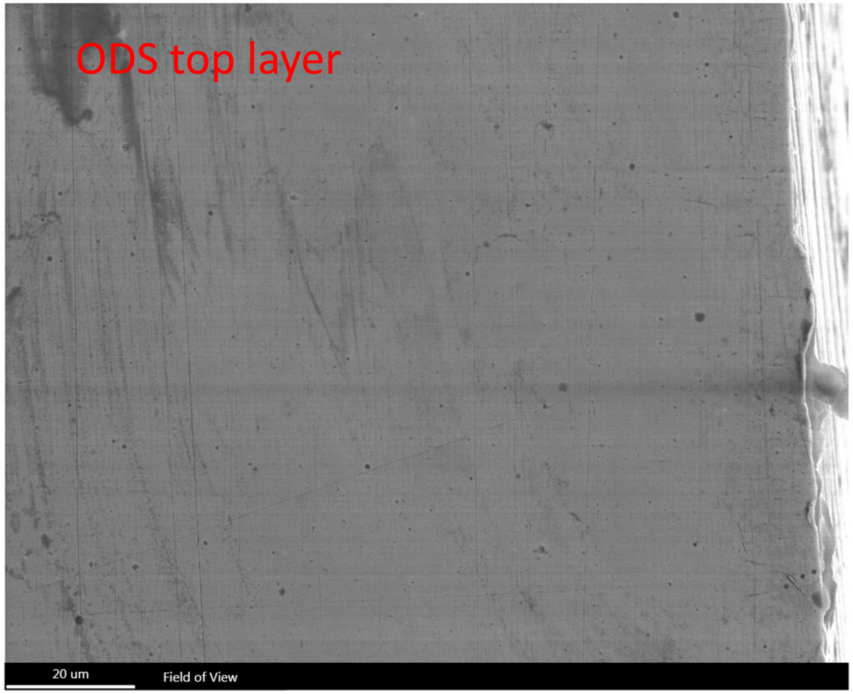

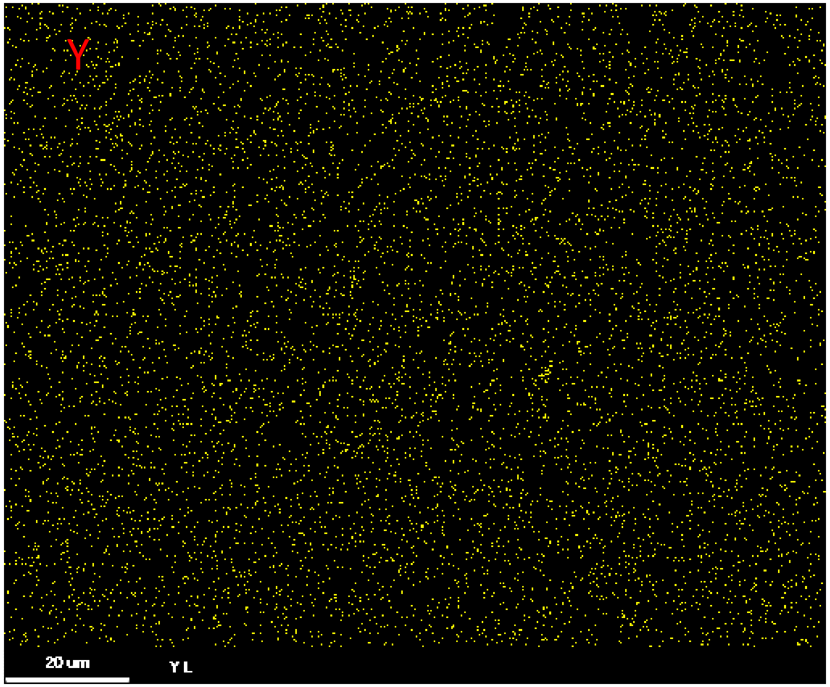

250W (BM+MCB) ODS, Top Layer

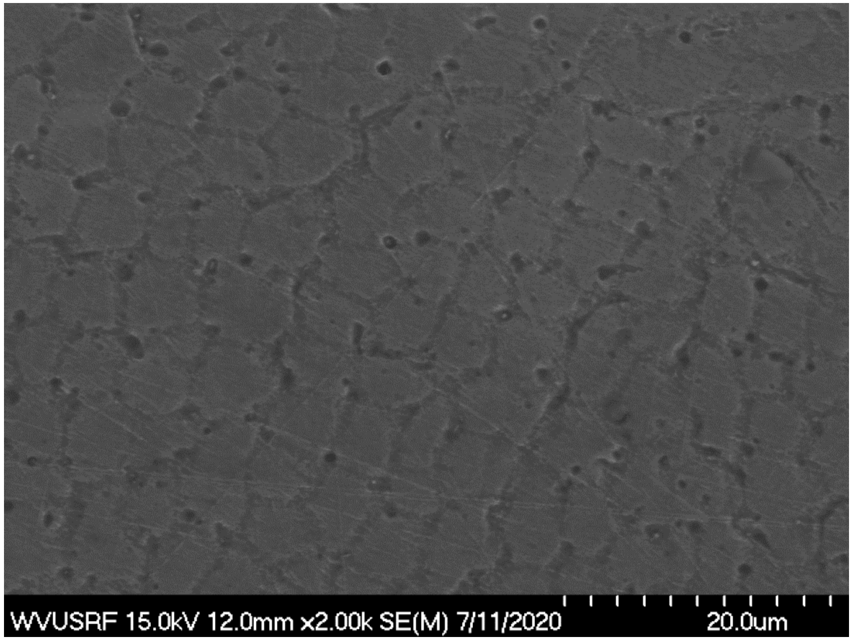

(a) Grain structure (<6 microns) , top layer

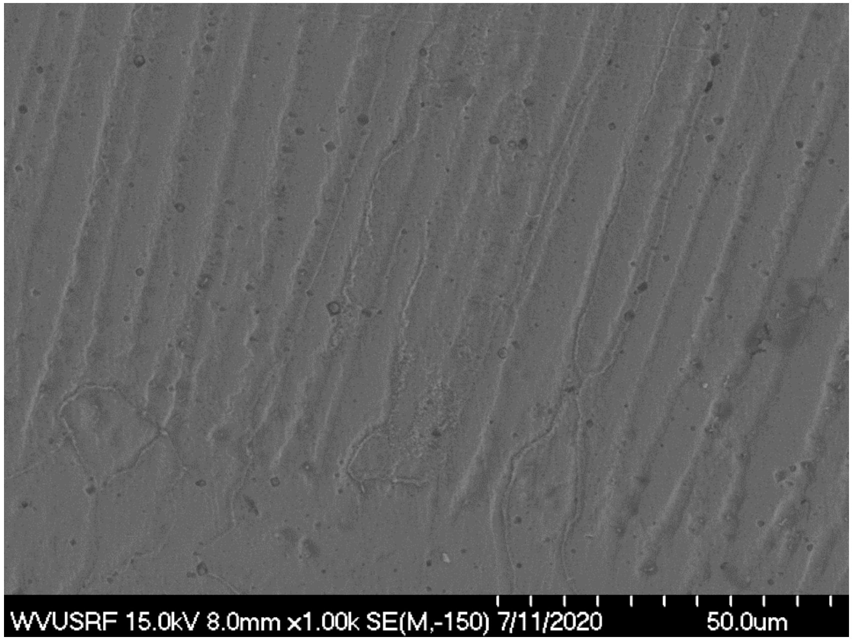

(b) Grain structure, interface

Initial Oxidation

Top view of oxide layer

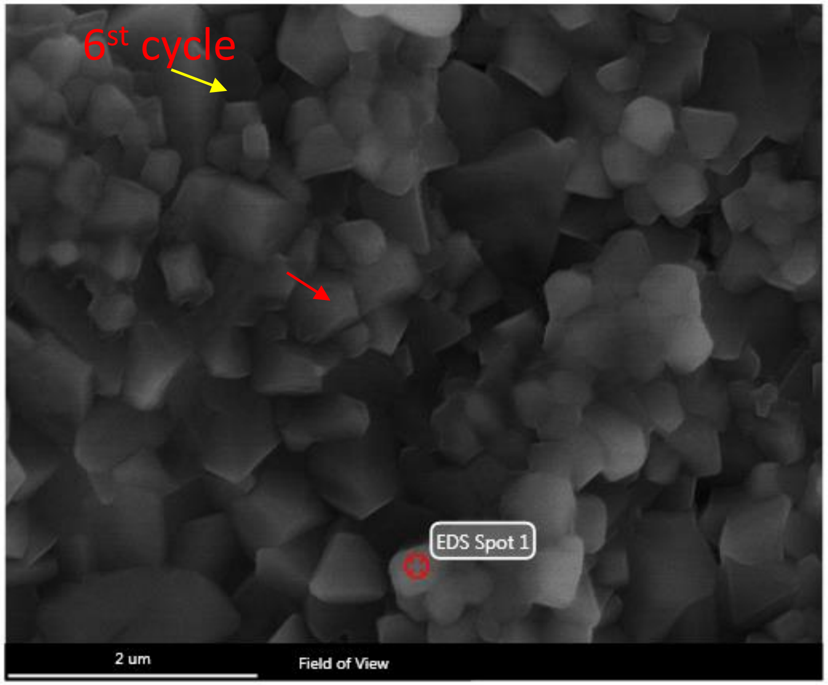

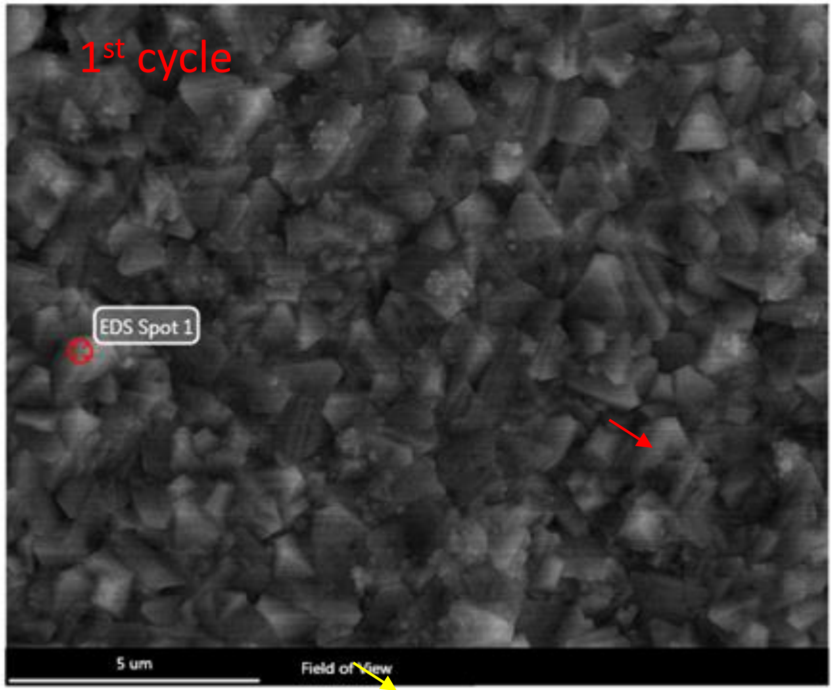

At 6th cycle, stable chromium oxide with oxides size less than 2 microns, an indication of continuous chromium oxide formation (red arrow) from 1st to 6th cycle. At initial oxidation, chromium oxide is the dominate oxide

Initial Oxidation

Top view of oxide layer

BM200- 16th cycle

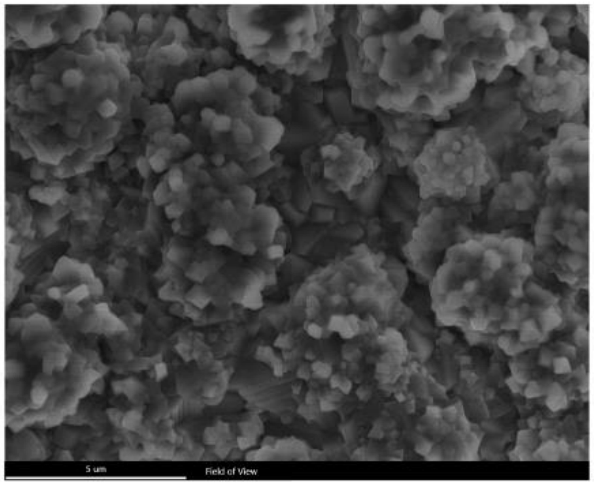

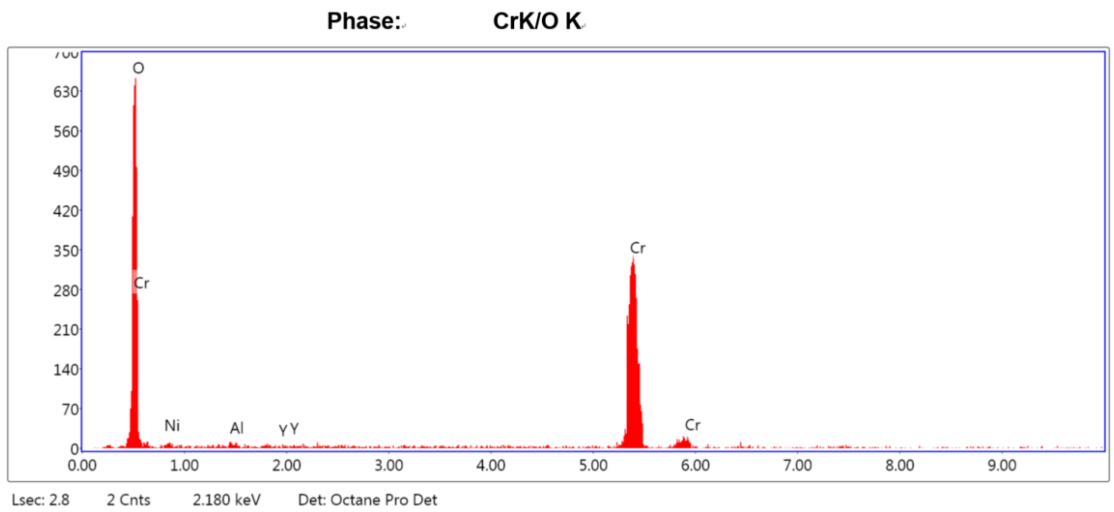

At the 16th cycle, EDS results indicate the main oxide is chromium oxide, smart quant results show the atomic% of O and Cr is 23.58% and 72.58% respectively.

In addition, Ni, Al, and Y were detected with the atomic % at 1.83%,0.58%, and 0.08% respectively. An indication of alumina formation.

eZAF Smart Quant Results

Element	Weight %	Atomic %	Net Int.	Error %	Kratio	Z	R	A	F
O K	23.58	50.08	1066.60	6.47	0.1938	1.2095	0.9068	0.6795	1.0000
AlK	0.46	0.58	20.60	36.59	0.0026	1.0744	0.9543	0.5175	1.0063
Y L	0.21	0.08	5.60	67.03	0.0016	0.8319	1.1310	0.8692	1.0237
CrK	72.58	47.43	1310.10	3.97	0.6899	0.9270	1.0209	1.0035	1.0218
NiK	3.16	1.83	24.60	32.44	0.0293	0.9256	1.0283	0.9562	1.0468

EDS of oxide layer at 16th cycle

***** Each cycle consists of moving test sample to the furnace within 15 minute and kept at 1100 ºC for 45 minutes and moved out within 15 minutes, kept for 45 minute at room temperature.***

Oxide layer stability

Continuous alumina, 80th cycle

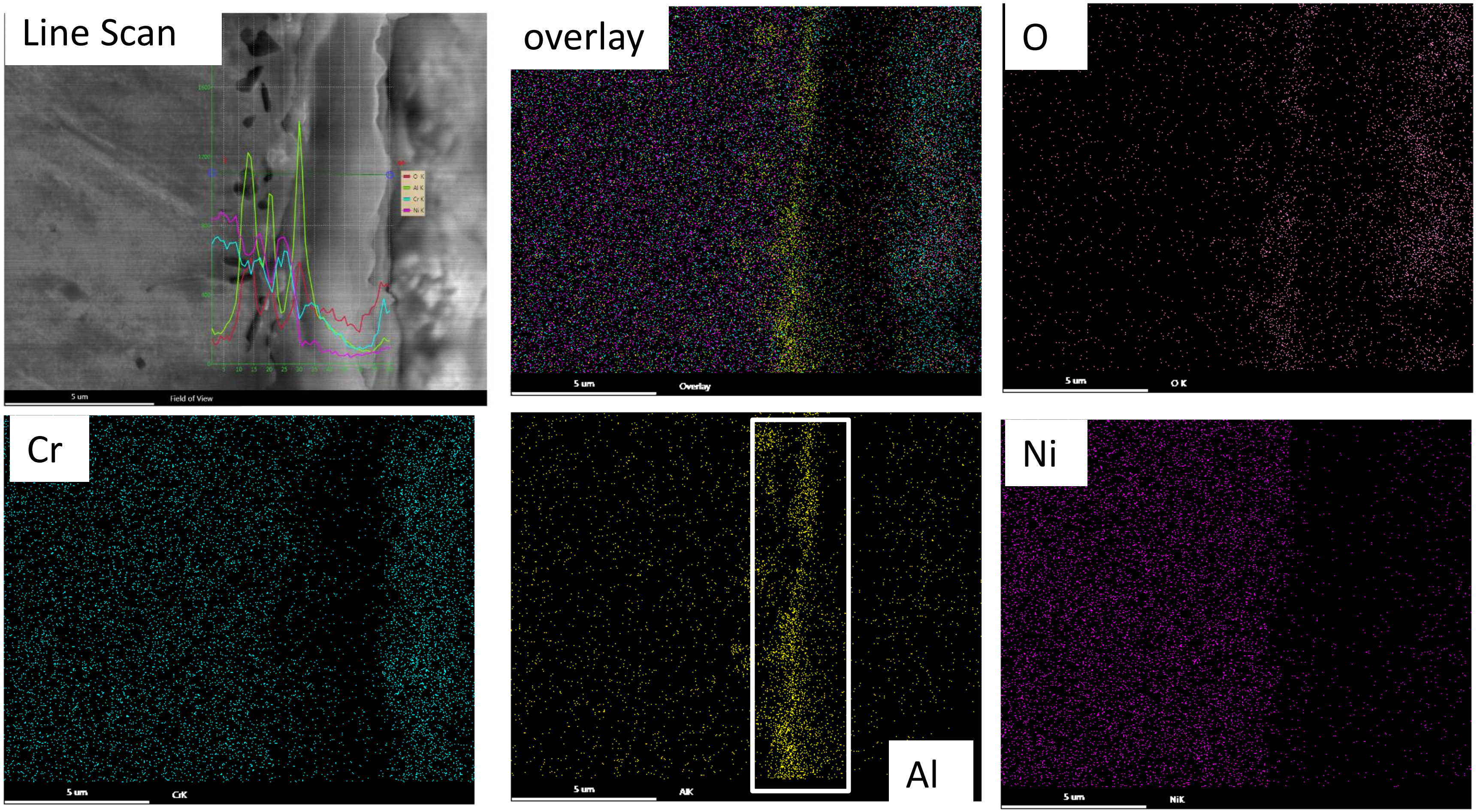

The Line Scan and mapping of cross section show that continues aluminum oxide layer formed underneath chromium oxide, very little Ni can be detected in oxide layer

Oxide layer stability

Continuous Alumina Formation (the 1280th cycle)

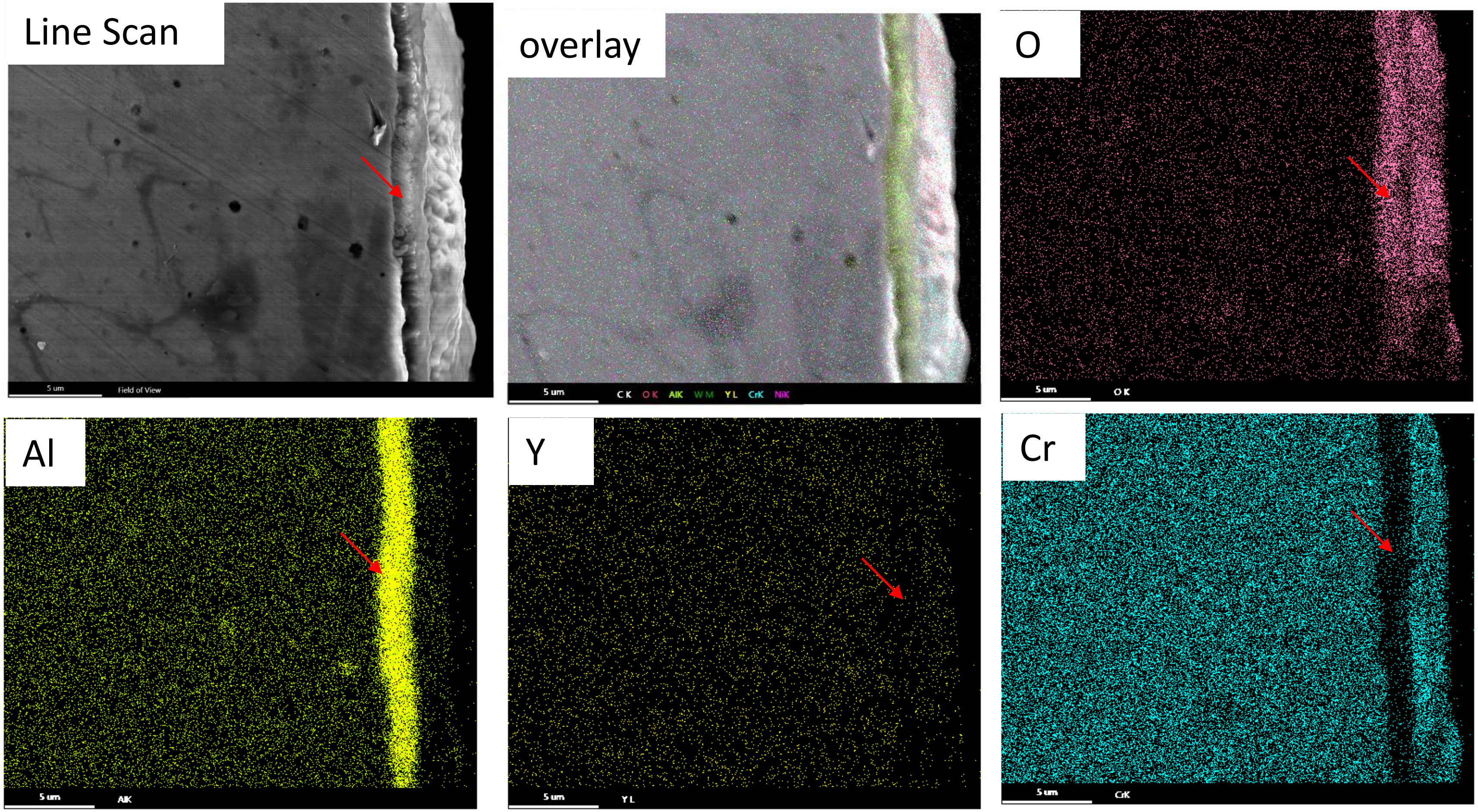

Continuous alumina (thickness: ~ 2 microns) at 1280 cycle, with chromium oxide on the top of it

Oxide layer stability

Oxide layer Formation (At the 4560 Cycle, Top View)

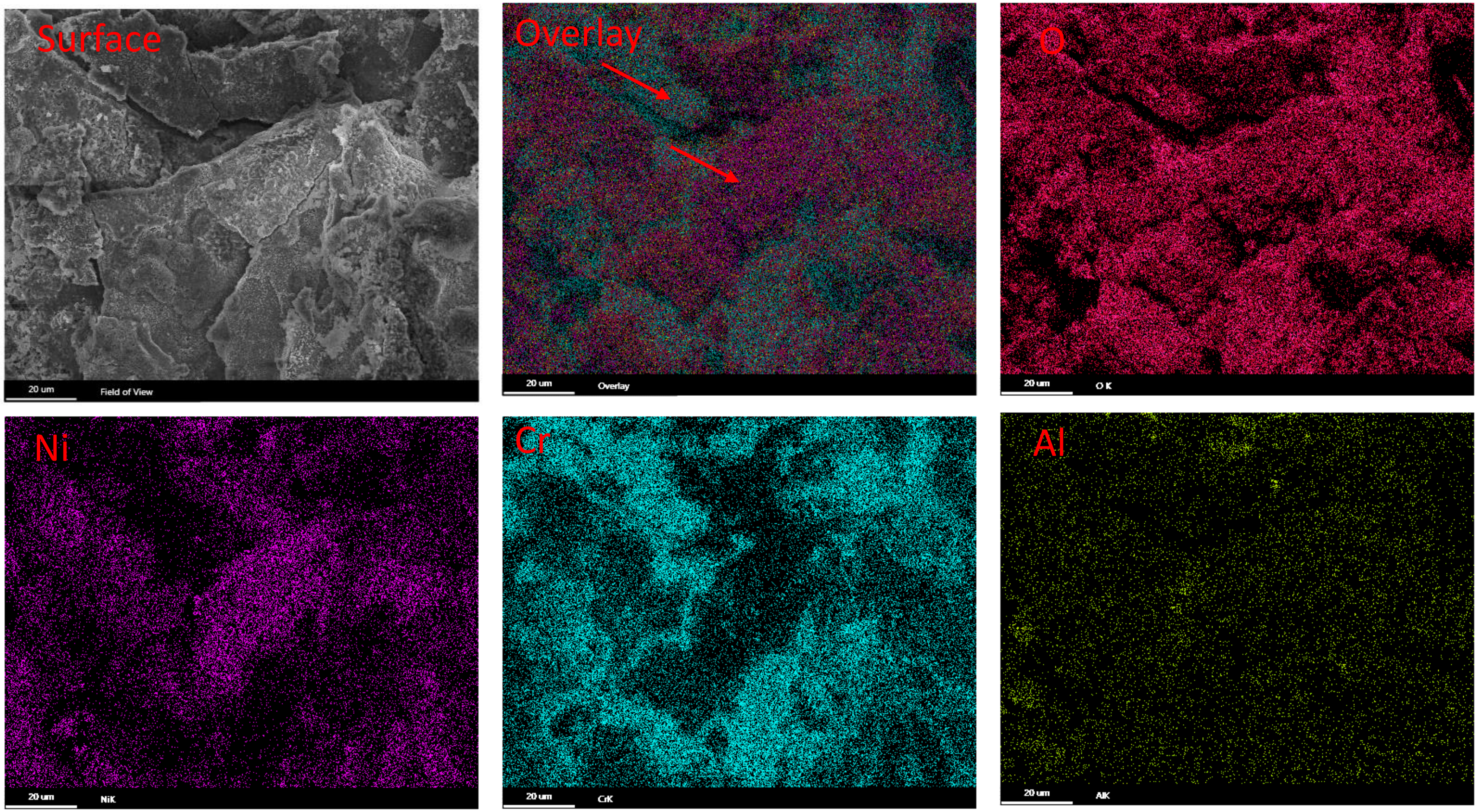

As shown in overlay, Nickel oxide with cracks is on the top of chromium oxide. Nickel and chromium oxide are still present after 4560 cycles. Near uniform Al indicated a continuous alumina layer beneath chromium oxide.

***** Each cycle consists of moving test sample to the furnace within 15 minute and kept at 1100 ^{o}C for 45 minutes and moved out within 15 minutes, kept for 45 minute at room temperature.***

Oxide layer stability

Oxide layer Formation (Cross section, 4560 Cycle)

At 4560 cycle, chromium oxide can be observed on the top of alumina, nickel oxide can not be detected an indication of spallation, typically, due to thermal expansion mismatch while cooling down during the thermal cyclic testing.

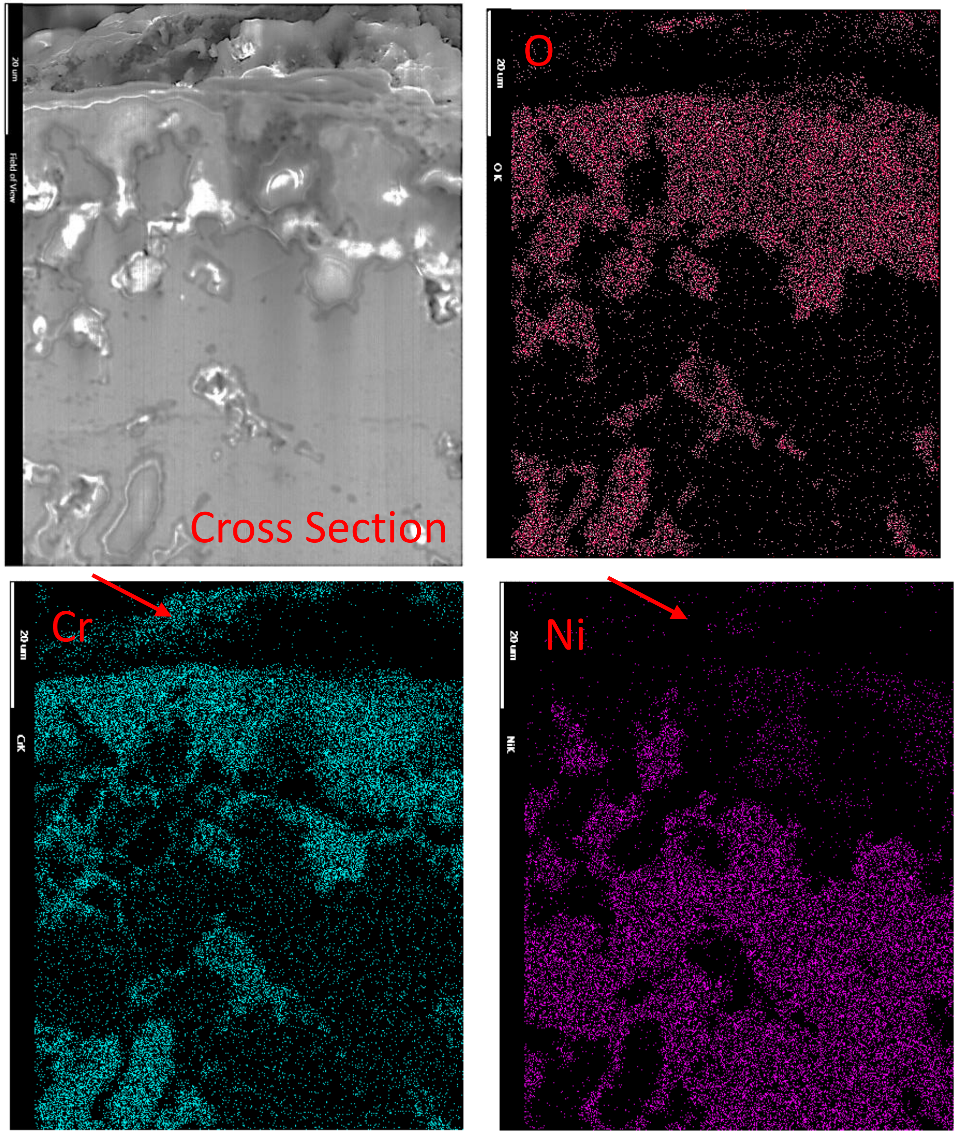

Oxide layer stability

Oxide layer Formation (Cross section at the 4560 Cycle)

EDS mapping indicates continuous alumina underneath chromium oxide at 4560 cycle.

Yttrium density in ODS coating is higher than that in oxide layer.

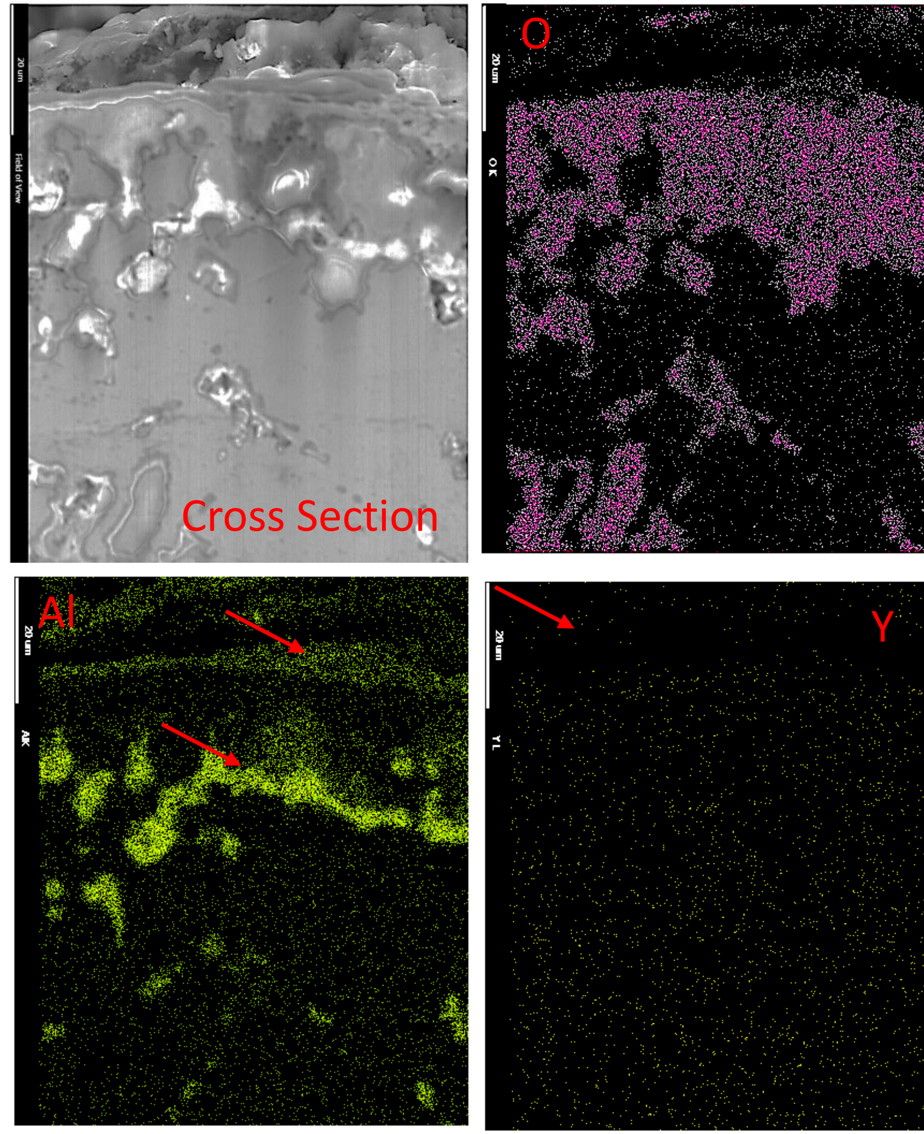

***** Each cycle consists of moving test sample to the furnace within 15 minute and kept at 1100 °C for 45 minutes and moved out within 15 minutes, kept for 45 minute at room temperature.***

Oxide layer stability

Oxide layer Formation (XRD at the 4560 Cycle)

At 4560 cycle, Al_2O_3,NiO, and Cr_2O_3 are detected, alumina is the dominate oxide.

Low intensity of Ni indicates spallation of NiO. $YAlO_3$ can be detected in oxide layer, i.e. Y-rich oxide particles would diffuse to alumina grain boundary to form Y-Al- rich nanoparticles.

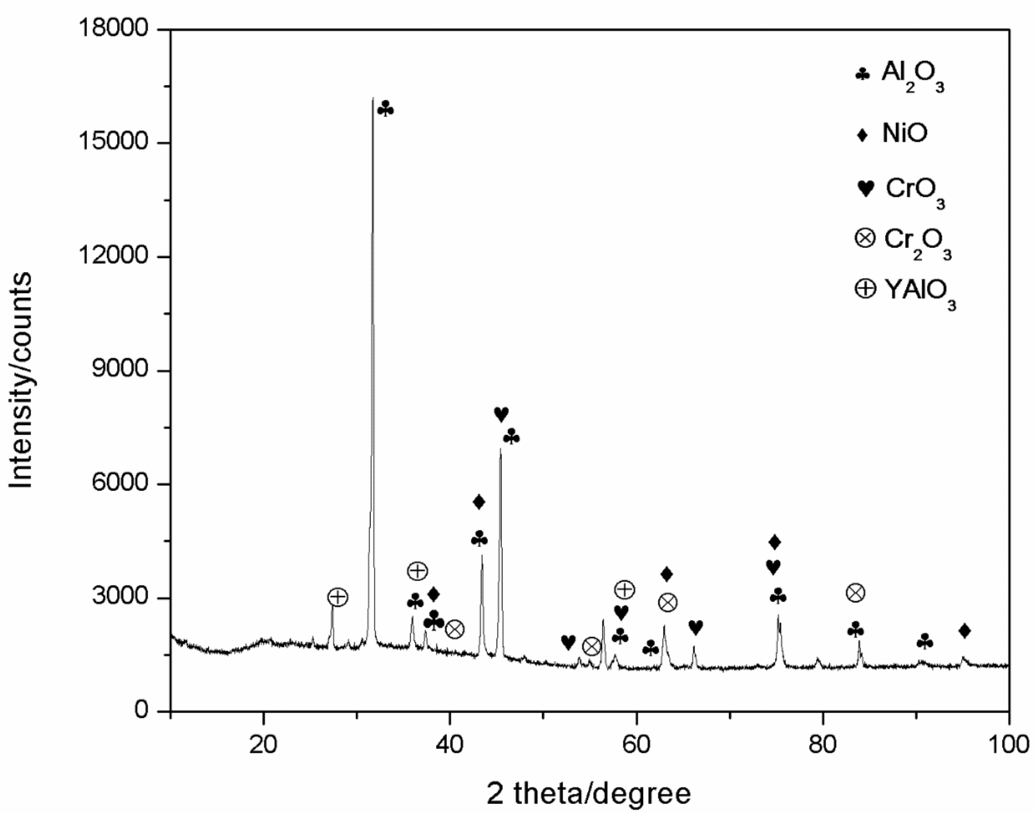

***** Each cycle consists of moving test sample to the furnace within 15 minute and kept at 1100 ºC for 45 minutes and moved out within 15 minutes, kept for 45 minute at room temperature.***

Schematic of Oxide Formation in ODS

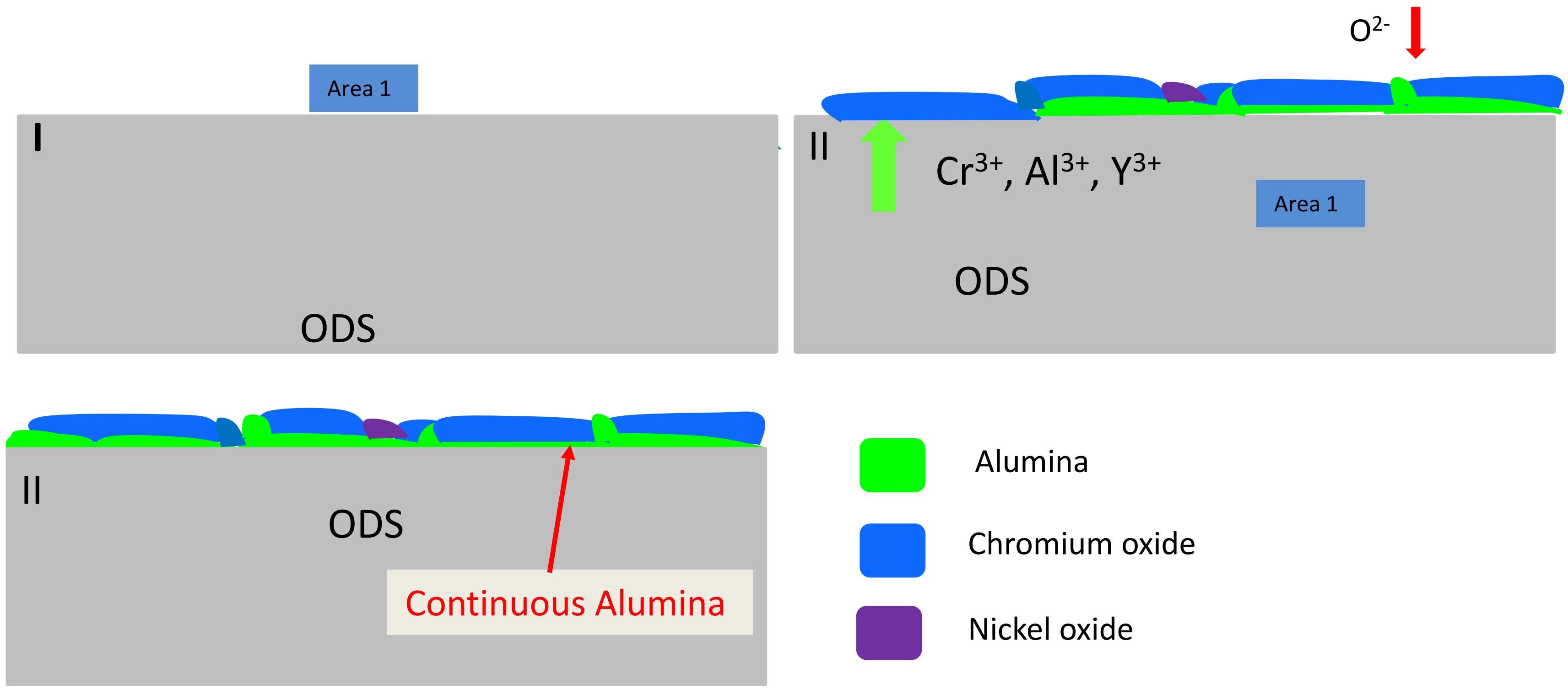

Stage I

At the early stage, chromium oxide formed first on the top of as-printed ODS.

Stage II

Alumina formed underneath chromium oxide, yttrium diffusion to oxide layer and formed Y-Al rich oxides

Stage III

Continuous alumina formed underneath chromium oxide

Thank You!